(1) A*0201-restricted epitope (amino acid 62-100)

origin	62	70	80	90	100
HXB2	GQLQPSLQTGSELER	SLYNTVATL	YCVHQRIEIKDTKEA		
IMS 1-28	E----A----------	-----I---	---------V------		
IMS 1-29	E----A----------	---------	---------V-----		
IMS 2-5	E----------------	----L----	-----K--VR-----		
IMS 4-24	-----A----------	--F----V-	-----K--V------		
IMS 6-34	-----A----------	---------	---------V-----		
IMS 7-11	A--H-A-K--------	-V-------	----------------		

(2) B51 restricted epitope (amino acid 310-348)

origin	310	320	330	340	348
HXB2	SQEVKNWMTETLLVQ	NANPDCKTI	LKALGPAATLEEMMT		
IMS 1-28	----------------	---------	----------------		
IMS 1-29	----------------	---------	----------------		
IMS 2-5	--D-------------	---------	----------------		
IMS 4-24	----------------	-S-----N-	----------------		
IMS 6-34	----------------	---------	----------------		
IMS 7-11	----------------	---------	----------------		

(3) A24-restricted epitope (amino acid 13-51)

origin	13	20	30	40	51
HXB2	LDRWEKIRLRPGGKK	KYKLKHIVW	ASRELERFAVNPGLL		
IMS 1-28	----------------	--R---L--	----------------		
IMS 1-29	----------------	--R------	----------------		
IMS 2-5	--K-------------	Q-R------	----------------		
IMS 4-24	----------------S-	--R------	----------------		
IMS 6-34	----------------	Q--------	----------------		
IMS 7-11	----------------	R-R---L--	----------------		

FIG. 2. Sequence variation in three CTL epitopes and their flanking regions. The amino acid sequences of six *gag* clones are shown. The reference sequence is derived from HXB2, and the differences are indicated. The numbering is done according to the HIV sequence database, Los Alamos National Laboratory, Los Alamos, N.Mex. The CTL epitope regions are boxed.

other target cells expressing different variants (Fig. 3e). Interestingly, IMS4-24 with Lys (K)-to-Ser (S) mutation at position 26 outside the epitope region was less well recognized than IMS1-29. We consistently observed this phenomenon in repeated experiments (data not shown).

CTL recognition of exogenously loaded variant peptides. To investigate whether the above findings of escape phenomenon from CTL killing were due to either loss of peptide binding to the MHC class I molecule or to the lack of TCR recognition, we prepared synthetic peptides that represented the variant epitopes and tested them for cross-recognition of the peptides in peptide titration assays by using the same CTL lines or clones that were used in experiments described for Fig. 3. To our surprise, A*0201-restricted CTL lines recognized the peptides of two A*0201-restricted CTL epitope variants, SVYNT VATL and SLFNTVAVL, which were not recognized by the CTLs when expressed endogenously. They recognized the SLFNTVAVL peptide less efficiently, with an SD_{50} of >100 nM (Fig. 4a). Target cells pulsed with SLYNLVATL peptide representing clone IMS 2-5 were not cross-recognized even at a saturated concentration (10 μM) (data not shown).

We also obtained similar discordant results in experiments of A24-restricted CTL epitope variants. A24-restricted 3R mutant-specific CTL lines recognized peptides of three variant s—KYRLKHLVW, RYRLKHLVW, and QYRLKHIVW—that were not recognized by the CTLs when they were expressed endogenously. In fact, the CTLs recognized QYRLKHIVW peptide even better than the 3R mutant peptide but did not cross-recognize the QYKLKHIVW peptide (Fig. 4b).

We tested one B*5101 variant peptide, NSNPDCKNI, in a peptide titration assay. This variant was not cross-recognized by any of the CTL clones even at a high concentration (1 μM) (Fig. 4c). The two amino acid mutations in this epitope coincided with two anchor residues to the MHC biding, suggesting that the lack of recognition of this variant was likely due to loss of peptide binding.

Mutations responsible for impairing the epitope processing and presentation. The discrepancies seen above between the CTL recognition of endogenously expressed and exogenously loaded antigen indicate that some mutations have caused the impairment of epitope processing and presentation. To locate specific variations that were responsible for the poor recognition of endogenously expressed HIV-1 *gag* variants, we constructed four different target vectors: an HXB2 *gag* sequence with A*0201-restricted epitope variations (SLFNTVAVL [HXB2-3F8V] or SVYNTVATL [HXB2-2V]) and IMS4-24- or IMS7-11-derived *gag* sequence with the wild-type A*0201 epitope sequence (IMS4-24-wild or IMS7-11-wild, respectively). The replacement of the variant epitope region with the

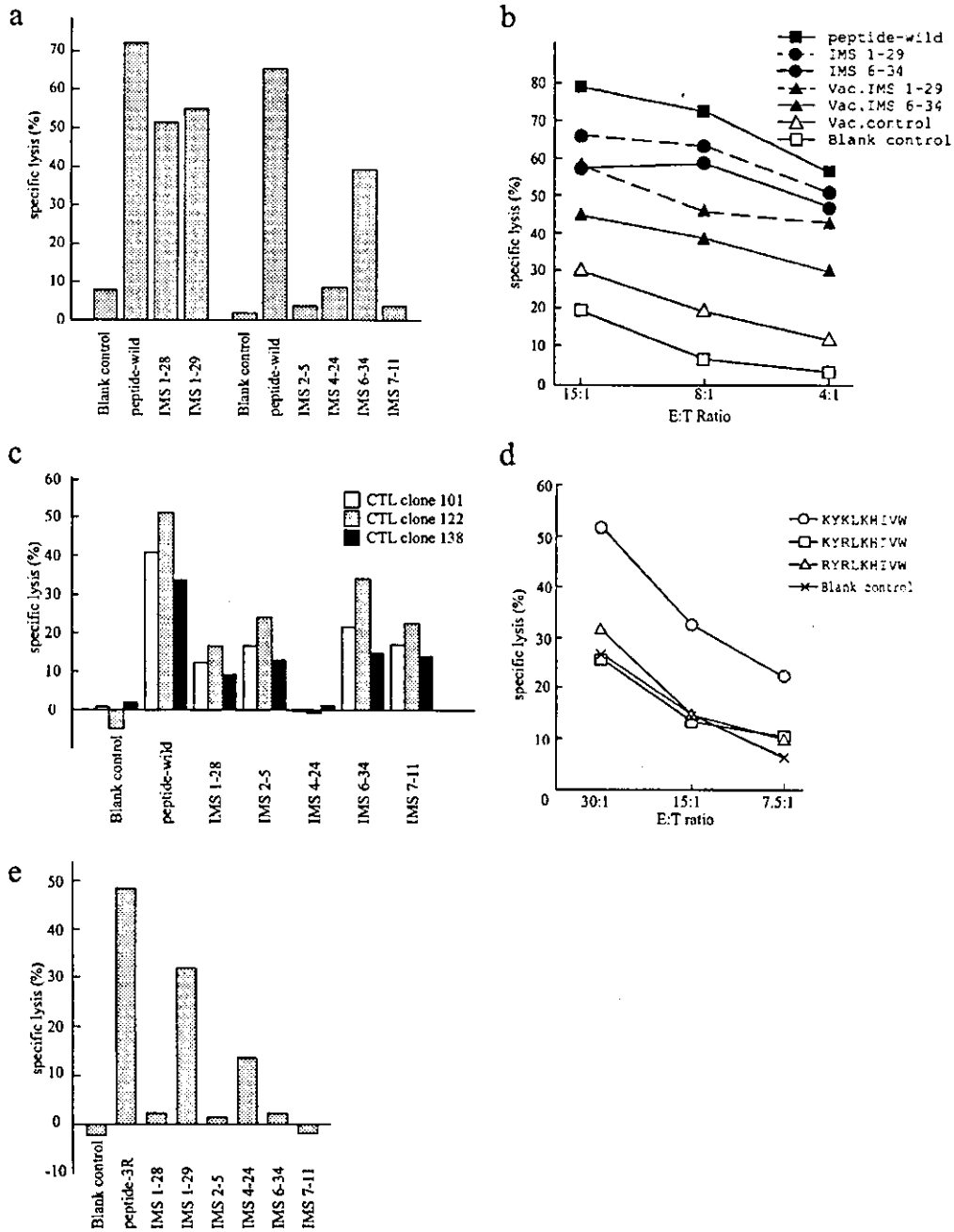

FIG. 3. (a) Specific lysis of A*0201-matched B-LCLs (HLA-A*0201/− and HLA-B*5101/−) producing Gag proteins of clinical isolates. Peptide target cells were pulsed with the A*0201 wild-type peptide, SLYNTVATL (10 μM). A*0201-restricted SLYNTVATL -specific CTL lines were induced from a single donor (IMS1). The E:T ratio was 10:1. This experiment was repeated, with a different B-LCLs (HLA-A*0201/31 and HLA-B27/*5101), giving the same pattern of recognition (data not shown). (b) Specific lysis of A*0201-matched B-LCLs (HLA-A*0201/− and HLA-B*5101/−) expressing *gag* clones of two clinical isolates with the VSV-G-pseudotyped HIV-1 vector versus recombinant vaccinia viruses. Recombinant vaccinia virus expressing the human CD4 gene was used as a vaccinia virus control (1). The effector and peptide target cells were prepared as described for panel a. (c) Specific lysis of B*5101-matched B-LCLs (HLA-A*0201/− and HLA-B*5101/−) producing the Gag proteins of five clones. Three B*5101-restricted NANPDCKTI -specific CTL clones were used as effector cells at an E:T ratio of 2:1 (23). The peptide target was pulsed with the B51 wild-type peptide NANPDCKI (1μM). (d) Specific lysis of A24-matched B-LCLs (HLA-A24/− and HLA-B46/52) pulsed with the peptides KYKLKHIVW, KYRLKHIVW, and RYRLKHIVW at 10 μM. A24-restricted, KYKLKHIVW -specific CTL lines were induced from one A24-positive donor. (e) Specific lysis of A24-matched B-LCLs (HLA-A24/− and HLA-B46/52) producing variant Gag proteins. A24-restricted KYRLKHIVW (3R)-specific CTL lines were induced from another A24-positive donor. The peptide target was pulsed with 3R mutant type peptide (10 μM). The E:T ratio was 20:1. The lysis of target cells without any peptide pulsing is shown as a blank control.

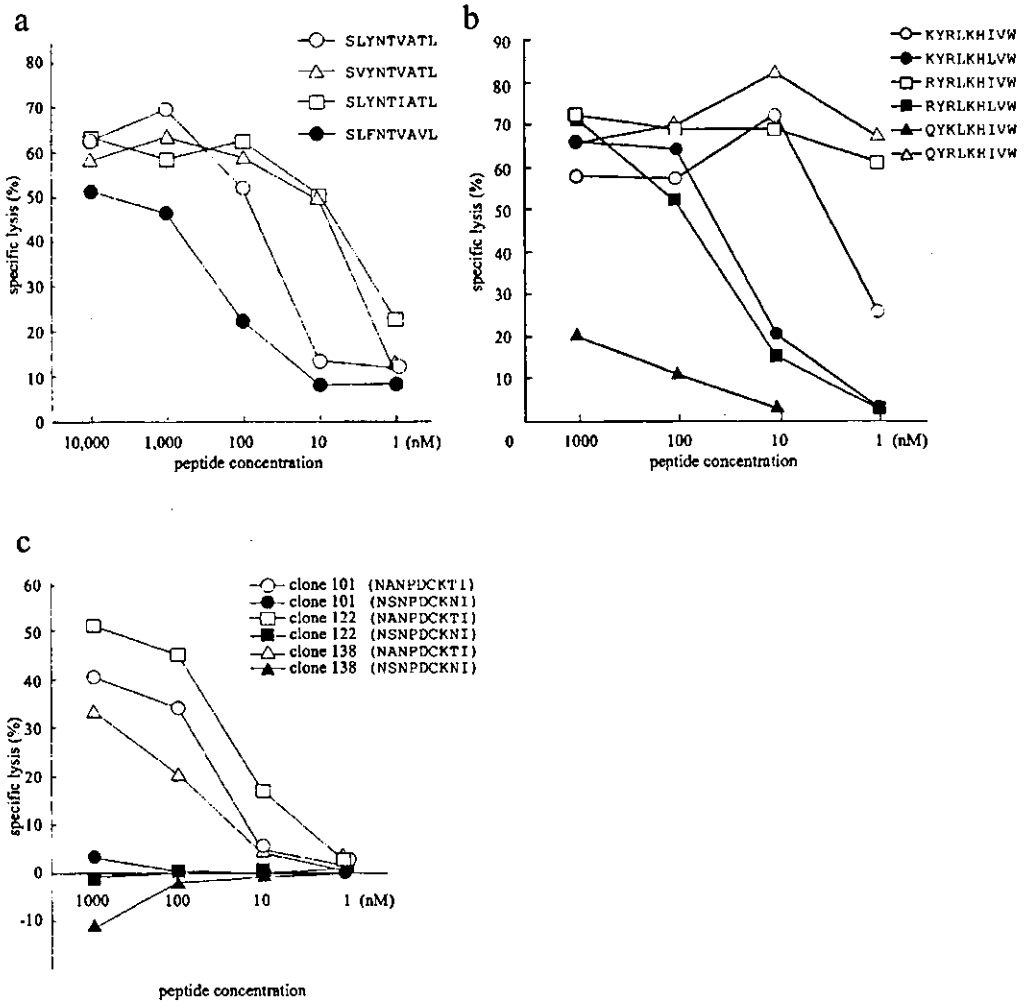

FIG. 4. Peptide titration assays. (a) Specific lysis of A*0201-matched B-LCLs pulsed with A*0201 variant peptides by A*0201-restricted CTLs at an E:T ratio of 20:1. (b) Specific lysis of A24-matched B-LCLs pulsed with 3R and its variant peptides by A24-restricted 3R mutant reactive CTLs at an E:T ratio of 20:1. (c) Specific lysis of B51-matched B-LCLs pulsed with B51 variant peptides by B51-restricted CTL clones at an E:T ratio of 2:1. The same effector and target cells were used as for Fig. 3. The percent lysis of the blank control has been subtracted.

wild-type epitope sequence restored CTL recognition of the escape variants, whereas replacement of the wild-type epitope with the two variant epitopes resulted in no CTL recognition of HXB2 Gag (Fig. 5a). The levels and patterns of Gag protein expression in target cells were analyzed by Western blot experiments (Fig. 5b). The expression levels of p55 Gag precursor and p24 CA did not significantly differ between the mutants and the wild type. The p17 MA band was not clear in HXB2-2V, IMS7-11-wild, and IMS4-24-wild, but the appearance of this band did not correlate with CTL killing. These results indicate that amino acid substitutions within the A*0201-restricted epitope region, rather than those in the flanking regions, have caused the inhibition of CTL recognition in our endogenous expression system.

To further investigate the effect of amino acid substitutions within the A24-restricted epitope on antigen processing and presentation, we introduced various point mutations into the wild-type HXB2 vector, pCTLpac, and tested them for the recognition by A24-restricted 3R mutant-reactive CTL lines. The A24-restricted 3R mutant-specific CTLs did not cross-recognize the wild-type peptide and the wild-type HXB2 vector but did recognize HXB2 with a 3R mutation (HXB2-1R). The substitution of Lys (K) with Arg (R) at position 28 (HXB2-1R3R) did not affect the A24-restricted 3R mutant-specific CTL recognition, but a Lys (K)-to-Gln (Q) substitution at position 28 (HXB2-1Q3R) or an Ile (I)-to-Leu (L) substitution at position 34 (HXB2-3R7L) resulted in the escape from CTL killing (Fig. 5c).

Replication kinetics of HIV-1 mutant viruses. We analyzed the replication kinetics of recombinant viruses carrying mutations that have affected the epitope processing and presentation by infecting H9 or Jurkat cells. All mutants were found to replicate to equivalent levels, suggesting that these mutations do not have a significant influence on HIV-1 replication (Fig. 6).

DISCUSSION

The present study focused on three Gag CTL epitopes restricted by three common HLA alleles in Japanese people (24).

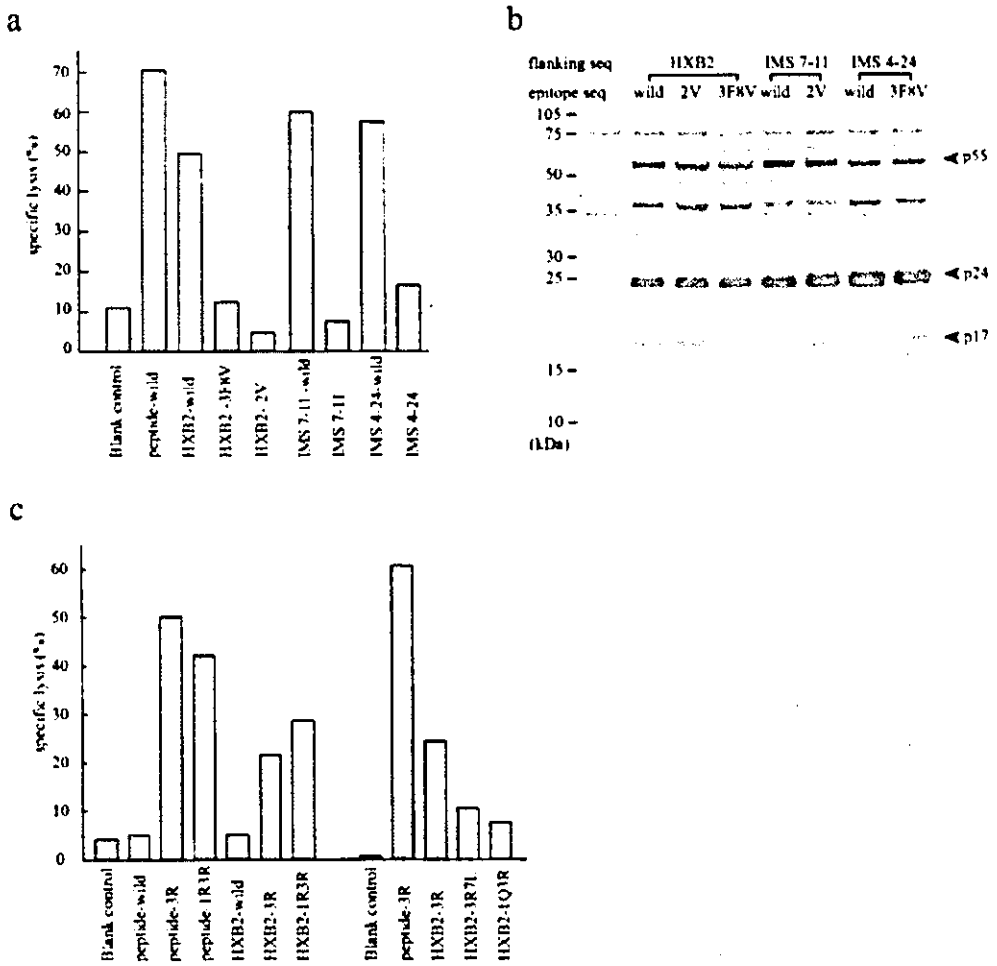

FIG. 5. (a) Specific lysis of A*0201-matched B-LCLs (HLA-A*0201/− and HLA-B*5101/−) that endogenously express chimeric *gag* clones bearing the variant CTL epitopes SLFNTVAVL and SVYNTVATL in the frame of HXB2 *gag* (HXB2-3F8V and HXB2-2V, respectively) or bearing the wild-type epitope in the frame of IMS7-11 and IMS4-24 Gag (IMS7-11-wild and IMS4-24-wild, respectively). A*0201-restricted SLYNTVATL CTL lines were induced from the same donor as for Fig. 3. Specific lysis of target cells expressing HXB2, IMS7-11, or IMS4-24 *gag* clones and being pulsed with the A*0201 wild-type peptide (10 μM) is shown in parallel. The E:T ratio was 20:1. (b) Levels and patterns of HIV-1 protein expression in target cells used in the experiments described for panel a. The Western blot was reacted with the serum from an HIV-1-infected individual. (c) Specific lysis of A24-matched B-LCLs (HLA A24/− and HLA-B46/52 or HLA-A24/26 and HLA-B51/52) that express *gag* clones with various point mutations. Point mutations were inserted into the A24-restricted CTL epitope region in the frame of wild-type HXB2 Gag (HXB2-wild): amino acid substitutions of Lys to Arg at position 30 (HXB2-3R) with Lys to Arg at position 28 (HXB2-1R3R), Ile to Lue at position 34 (HXB2-3R7L), or Lys to Gln at position 28 (HXB2-1Q3R). Peptide target cells were pulsed with either the KYRLKHIVW (3R) or the RYRLKHIVW (1R3R) mutant peptide at 10 μM. The effector cells were A24-restricted 3R mutant-specific CTL lines from the same donor as in the Fig. 3e experiment. The E:T ratio was 20:1.

The Gag protein is most commonly targeted by CTL-inducing HIV/AIDS vaccines (15). In our endogenous expression system, three A*0201-restricted epitope variants and one B*5101-restricted epitope variant escaped from the wild-type CTL recognition, and four A24-restricted epitope variants escaped from the A24-restricted 3R mutant-reactive CTL recognition. Intriguingly, two A*0201-restricted variants and three A24-restricted variants escaped from CTL killing when the *gag* clones were expressed endogenously in the target cells by the HIV-1 vector, despite the fact that the synthetic variant peptides were well recognized by the CTLs when loaded onto the MHC class I molecule exogenously. The peptide titration experiments have revealed that the strength of these variant peptides' recognition was almost equivalent to that of the A*0201-restricted wild-type peptide or the A24-restricted 3R mutant peptide. The results were not likely due to differences in the pattern of Gag protein expression, as shown in the Western blot experiments. All target cells were confirmed to express a sufficient level of Gag protein by p24 antigen production. Therefore, we believe that the escape mechanism of these variants resides in the antigen processing and presentation, as has been observed in a mouse model with murine leukemia virus infection (19). The observation of such phenomenon in two epitopes restricted by different alleles implies that this finding is not unique to a particular epitope-MHC pair.

Since all variants investigated here were derived from clinical samples and those mutations did not affect the virus replication, our observations are relevant for discussing what may be going on in HIV-infected individuals. Our results indicate

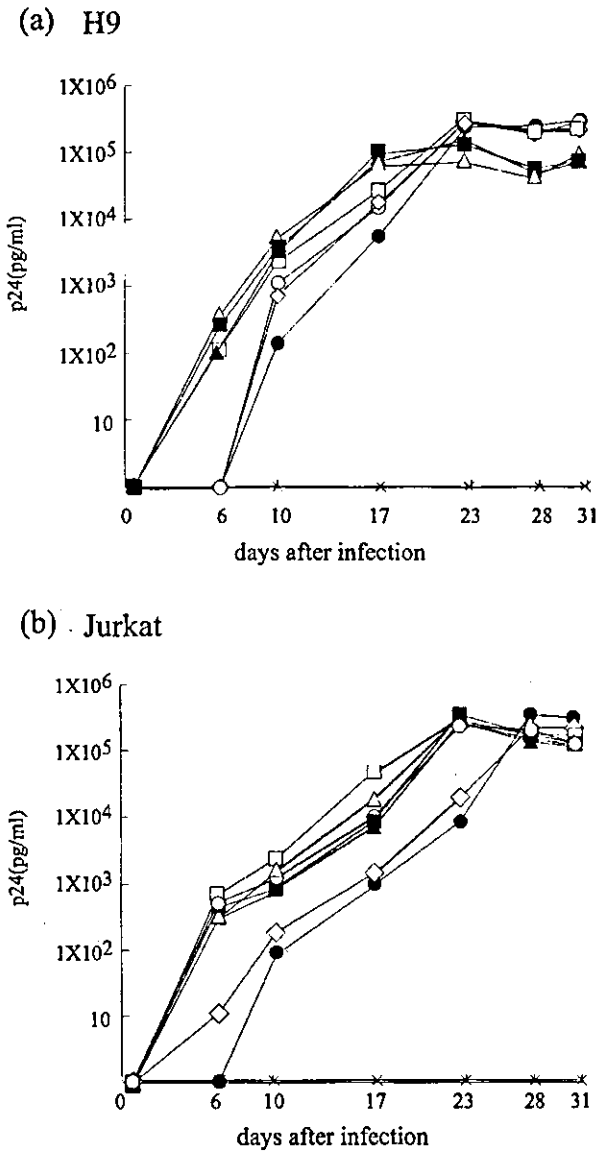

FIG. 6. Replication of HIV-1 clones with mutations that impaired the processing and presentation of A*0201 or A24 CTL epitopes in H9 (a) and Jurkat (b) cells. The kinetics of each recombinant virus replication were monitored as the production of p24 antigen by p24 ELISA. Symbols: ○, wild-type; □, A24-3R; ■, A24-K26S+3R; △, A24-3R7L; ▲, A24-1Q3R; ●, A*0201-3F8V; ◇, A*0201-2V; ×, mock.

that the impaired antigen processing and presentation often occurs in HIV-1 field isolates and thus is one of the major mechanisms that enable HIV-1 to escape from the CTL recognition. To understand further the significance of this escape mechanism, it is important to evaluate an accumulation of such escape variants in infected hosts in a longitudinal study or at a population level. A previous report using a vaccinia virus expression system did not reveal that any mutations in the A*0201-restricted p17 epitope of HIV-1 and its flanking region altered the processing and presentation of its variant epitope (4). However, that study did not investigate A*0201-restricted 2V and 3F8V variants, which we found affected epitope processing and presentation.

Experiments with chimeric genes, as well as point mutations, showed that escapes from epitope processing and presentation were mostly attributable to mutations within the epitope regions rather than its flanking regions. In the present study, we demonstrated that point mutations of Lys (L) to Gln (Q) at position 28 and of Ile to Leu at position 34 drastically impaired the processing and presentation of the A24-restricted CTL epitope. Moreover, the experiment with HXB2 clone carrying IMS 7-11 variant of A*0201-restricted CTL epitope indicates that a substitution of Leu (L) to Val (V) at position 78 was responsible for the impaired processing and presentation of the epitope. These mutations in the epitope region may have induced a proteasome cleavage site within the epitope (19). On the other hand, we observed that the variations in the 15 amino acids up- and downstream of the epitope did not affect CTL recognition. An exception was a Lys (L)-to-Ser (S) substitution (−2S) at position 26, which is only two amino acids adjacent to the N terminus of the A24-restricted epitope. However, this −2S substitution did not void the A24-restricted 3R mutant-reactive CTL recognition completely. One possible explanation is that the −2S substitution shifted the optimal proteasome cleavage site, resulting in the generation of a larger peptide, which has a lower affinity to the MHC class I molecule.

We have first attempted to investigate the antigen processing and presentation by the conventional recombinant vaccinia virus method for all variants before we established this VSV-G-pseudotyped HIV-1 vector method. Soon, we realized that preparing recombinant vaccinia viruses was much more laborious and time-consuming. Early experiments of comparing two methods by using the first available recombinant vacinia viruses concluded that the HIV-1 vector method demonstrated CTL killing better than did the recombinant vaccinia virus method (Fig. 3b). In the recombinant vaccinia virus expression system, the massive production of vaccinia virus proteins inevitably takes place, along with the expression of an HIV-1 gene and sometimes causes a high background lysis. The expression manner and the production ratio to non-HIV proteins may also influence antigen processing and presentation (27, 34). Thus, we thought that the antigen processing and presentation in the HIV-1 vector expression system is more physiological than the recombinant vaccinia virus expression system and that continuing vaccinia virus experiments would not be significantly beneficial to address the issue of antigen processing and presentation. Nevertheless, there remains a concern that there might be a potential difference in the antigen processing and presentation between immortalized B cells that were used here and primary $CD4^+$ T cells (32, 33). Perhaps it is important to reevaluate the interaction of CTLs and these variants in experiments with variant HIV-1-infected T cells. Our HIV-1 vector carries neither the *nef* gene nor the *vpu* gene, which significantly affect antigen presentation by downregulating MHC class I cell surface expression (5, 13). From this point of view, one might expect that more variants would escape from the CTL recognition in the actual HIV-1 infection than what is shown in our experiments. However, we think that our system is suited to identify a specific association between a certain mutation and the escape from antigen processing and presentation. To prove the existence of this mode of escape mecha-

nism, we may need a new system that can directly detect a trace of specific epitopes that are eluted from MHC class I molecules of HIV-1 antigen-producing cells.

Although the structure analysis of MHC class I molecules and its binding motif has facilitated the prediction of CTL epitopes from the primary amino acid sequence data of HIV-1 (6, 11, 26), it remains difficult to envisage the efficiency of epitope processing and presentation. Enormous diversity realized in HIV-1 field isolates causes a further complexity (7). Our data emphasize the importance of testing HIV-1 variants in an endogenous expression system. Detailed analysis of epitope processing and presentation among HIV-1 field isolates, particularly of non-B subtypes circulating in the vaccine trial fields, is essential, since such information allows us to forecast which virus may elude the immunity elicited by vaccines, thus providing a clue for a rational design for effective HIV/AIDS vaccines.

ACKNOWLEDGMENTS

We thank the donors in this study for their participation, Sachiko Tateishi for assistance, and Kunito Yoshiike for critical reading of the manuscript.

This study was supported by the Japanese Ministry of Health, Labor, and Welfare and the Japan Health Science Foundation.

REFERENCES

1. **Aoki, N., T. Shioda, H. Satoh, and H. Shibuta.** 1991. Syncytium formation of human and non-human cells by recombinant vaccinia viruses carrying the HIV *env* gene and human CD4 gene. AIDS 5:871–875.
2. **Barouch, D. H., J. Kunstman, M. J. Kuroda, J. E. Schmitz, S. Santra, F. W. Peyerl, G. R. Krivulka, K. Beaudry, M. A. Lifton, D. A. Gorgone, D. C. Montefiori, M. G. Lewis, S. M. Wolinsky, and N. L. Letvin.** 2002. Eventual AIDS vaccine failure in a rhesus monkey by viral escape from cytotoxic T lymphocytes. Nature 415:335–339.
3. **Borrow, P., H. Lewicki, X. Wei, M. S. Horwitz, N. Peffer, H. Meyers, J. A. Nelson, J. E. Gairin, B. H. Hahn, M. B. Oldstone, and G. M. Shaw.** 1997. Antiviral pressure exerted by HIV-1-specific cytotoxic T lymphocytes (CTLs) during primary infection demonstrated by rapid selection of CTL escape virus. Nat. Med. 3:205–211.
4. **Brander, C., O. O. Yang, N. G. Jones, Y. Lee, P. Goulder, R. P. Johnson, A. Trocha, D. Colbert, C. Hay, S. Buchbinder, C. C. Bergmann, H. J. Zweerink, S. Wolinsky, W. A. Blattner, S. A. Kalams, and B. D. Walker.** 1999. Efficient processing of the immunodominant, HLA-A*0201-restricted human immunodeficiency virus type 1 cytotoxic-T-lymphocyte epitope despite multiple variations in the epitope flanking sequences. J. Virol. 73:10191–10198.
5. **Collins, K. L., B. K. Chen, S. A. Kalams, B. D. Walker, and D. Baltimore.** 1998. HIV-1 Nef protein protects infected primary cells against killing by cytotoxic T lymphocytes. Nature 391:397–401.
6. **Falk, K., O. Rotzschke, S. Stevanovic, G. Jung, and H. G. Rammensee.** 1991. Allele-specific motifs revealed by sequencing of self-peptides eluted from MHC molecules. Nature 351:290–296.
7. **Gaschen, B., J. Taylor, K. Yusim, B. Foley, F. Gao, D. Lang, V. Novitsky, B. Haynes, B. H. Hahn, T. Bhattacharya, and B. Korber.** 2002. Diversity considerations in HIV-1 vaccine selection. Science 296:2354–2360.
8. **Goulder, P. J., R. E. Phillips, R. A. Colbert, S. McAdam, G. Ogg, M. A. Nowak, P. Giangrande, G. Luzzi, B. Morgan, A. Edwards, A. J. McMichael, and S. Rowland-Jones.** 1997. Late escape from an immunodominant cytotoxic T-lymphocyte response associated with progression to AIDS. Nat. Med. 3:212–217.
9. **Ho, D. D., A. U. Neumann, A. S. Perelson, W. Chen, J. M. Leonard, and M. Markowitz.** 1995. Rapid turnover of plasma virions and CD4 lymphocytes in HIV-1 infection. Nature 373:123–126.
10. **Hoshikawa, N., A. Kojima, A. Yasuda, E. Takayashiki, S. Masuko, J. Chiba, T. Sata, and T. Kurata.** 1991. Role of the gag and pol genes of human immunodeficiency virus in the morphogenesis and maturation of retrovirus-like particles expressed by recombinant vaccinia virus: an ultrastructural study. J. Gen. Virol. 72:2509–2517.
11. **Ikeda-Moore, Y., H. Tomiyama, M. Ibe, S. Oka, K. Miwa, Y. Kaneko, and M. Takiguchi.** 1998. Identification of a novel HLA-A24-restricted cytotoxic T-lymphocyte epitope derived from HIV-1 Gag protein. AIDS 12:2073–2074.
12. **Kawana, A., H. Tomiyama, M. Takiguchi, T. Shioda, T. Nakamura, and A. Iwamoto.** 1999. Accumulation of specific amino acid substitutions in HLA-B35-restricted human immunodeficiency virus type 1 cytotoxic T lymphocyte epitopes. AIDS Res. Hum. Retrovir. 15:1099–1107.
13. **Kerkau, T., I. Bacik, J. R. Bennink, J. W. Yewdell, T. Hunig, A. Schimpl, and U. Schubert.** 1997. The human immunodeficiency virus type 1 (HIV-1) Vpu protein interferes with an early step in the biosynthesis of major histocompatibility complex (MHC) class I molecules. J. Exp. Med. 185:1295–1305.
14. **Koenig, S., A. J. Conley, Y. A. Brewah, G. M. Jones, S. Leath, L. J. Boots, V. Davey, G. Pantaleo, J. F. Demarest, C. Carter, et al.** 1995. Transfer of HIV-1-specific cytotoxic T lymphocytes to an AIDS patient leads to selection for mutant HIV variants and subsequent disease progression. Nat. Med. 1:330–336.
15. **McMichael, A. J., and T. Hanke.** 2003. HIV vaccines 1983–2003. Nat. Med. 9:874–880.
16. **McMichael, A. J., and S. L. Rowland-Jones.** 2001. Cellular immune responses to HIV. Nature 410:980–987.
17. **Momburg, F., and G. J. Hammerling.** 1998. Generation and TAP-mediated transport of peptides for major histocompatibility complex class I molecules. Adv. Immunol. 68:191–256.
18. **Moore, C. B., M. John, I. R. James, F. T. Christiansen, C. S. Witt, and S. A. Mallal.** 2002. Evidence of HIV-1 adaptation to HLA-restricted immune responses at a population level. Science 296:1439–1443.
19. **Ossendorp, F., M. Eggers, A. Neisig, T. Ruppert, M. Groettrup, A. Sijts, E. Mengede, P. M. Kloetzel, J. Neefjes, U. Koszinowski, and C. Melief.** 1996. A single residue exchange within a viral CTL epitope alters proteasome-mediated degradation resulting in lack of antigen presentation. Immunity 5:115–124.
20. **Phillips, R. E., S. Rowland-Jones, D. F. Nixon, F. M. Gotch, J. P. Edwards, A. O. Ogunlesi, J. G. Elvin, J. A. Rothbard, C. R. Bangham, C. R. Rizza, et al.** 1991. Human immunodeficiency virus genetic variation that can escape cytotoxic T-cell recognition. Nature 354:453–459.
21. **Price, D. A., P. J. Goulder, P. Klenerman, A. K. Sewell, P. J. Easterbrook, M. Troop, C. R. Bangham, and R. E. Phillips.** 1997. Positive selection of HIV-1 cytotoxic T lymphocyte escape variants during primary infection. Proc. Natl. Acad. Sci. USA 94:1890–1895.
22. **Ratner, L., A. Fisher, L. L. Jagodzinski, H. Mitsuya, R. S. Liou, R. C. Gallo, and F. Wong-Staal.** 1987. Complete nucleotide sequences of functional clones of the AIDS virus. AIDS Res. Hum. Retrovir. 3:57–69.
23. **Rock, K. L., and A. L. Goldberg.** 1999. Degradation of cell proteins and the generation of MHC class I-presented peptides. Annu. Rev. Immunol. 17: 739–779.
24. **Saito, S., S. Ota, E. Yamada, H. Inoko, and M. Ota.** 2000. Allele frequencyes and haplotypic associations defined by allelic DNA typing at HLA class I and class II loci in the Japanese population. Tissue Antigens 56:522–529.
25. **Sugiura, W., Z. Matsuda, Y. Yokomaku, K. Hertogs, B. Larder, T. Oishi, A. Okano, T. Shiino, M. Tatsumi, M. Matsuda, H. Abumi, N. Takata, S. Shirahata, K. Yamada, H. Yoshikura, and Y. Nagai.** 2002. Interference between D30N and L90M in selection and development of protease inhibitor-resistant human immunodeficiency virus type 1. Antimicrob. Agents Chemother. 46:708–715.
26. **Tomiyama, H., T. Sakaguchi, K. Miwa, S. Oka, A. Iwamoto, Y. Kaneko, and M. Takiguchi.** 1999. Identification of multiple HIV-1 CTL epitopes presented by HLA-B*5101 molecules. Hum. Immunol. 60:177–186.
27. **Tsomides, T. J., A. Aldovini, R. P. Johnson, B. D. Walker, R. A. Young, and H. N. Eisen.** 1994. Naturally processed viral peptides recognized by cytotoxic T lymphocytes on cells chronically infected by human immunodeficiency virus type 1. J. Exp. Med. 180:1283–1293.
28. **Tsomides, T. J., B. D. Walker, and H. N. Eisen.** 1991. An optimal viral peptide recognized by CD8$^-$ T cells binds very tightly to the restricting class I major histocompatibility complex protein on intact cells but not to the purified class I protein. Proc. Natl. Acad. Sci. USA 88:11276–11280.
29. **Van Baalen, C. A., M. Schutten, R. C. Huisman, P. H. Boers, R. A. Gruters, and A. D. Osterhaus.** 1998. Kinetics of antiviral activity by human immunodeficiency virus type 1-specific cytotoxic T lymphocytes (CTL) and rapid selection of CTL escape virus in vitro. J. Virol. 72:6851–6857.
30. **Wei, X., S. K. Ghosh, M. E. Taylor, V. A. Johnson, E. A. Emini, P. Deutsch, J. D. Lifson, S. Bonhoeffer, M. A. Nowak, B. H. Hahn, et al.** 1995. Viral dynamics in human immunodeficiency virus type 1 infection. Nature 373: 117–122.
31. **Wei, X., J. M. Decker, S. Wang, H. Hui, J. C. Kappes, X. Wu, J. F. Salazar-Gonzalez, M. G. Salazar, J. M. Kilby, M. S. Saag, N. L. Komarova, M. A. Nowak, B. H. Hahn, P. D. Kwong, and G. M. Shaw.** 2003. Antibody neutralization and escape by HIV-1. Nature 422:307–312.
32. **Yang, O. O., S. A. Kalams, M. Rosenzweig, A. Trocha, N. Jones, M. Koziel, B. D. Walker, and R. P. Johnson.** 1996. Efficient lysis of human immunodeficiency virus type 1-infected cells by cytotoxic T lymphocytes. J. Virol. 70:5799–5806.
33. **Yang, O. O., S. A. Kalams, A. Trocha, H. Cao, A. Luster, R. P. Johnson, and B. D. Walker.** 1997. Suppression of human immunodeficiency virus type 1 replication by CD8$^+$ cells: evidence for HLA class I-restricted triggering of cytolytic and noncytolytic mechanisms. J. Virol. 71:3120–3128.
34. **Yewdell, J. W., and J. R. Bennink.** 1999. Immunodominance in major histocompatibility complex class I-restricted T lymphocyte responses. Annu. Rev. Immunol. 17:51–88.

Phenotypic classification of human CD8+ T cells reflecting their function: inverse correlation between quantitative expression of CD27 and cytotoxic effector function

Hiroko Tomiyama, Hiroshi Takata, Tomoko Matsuda and Masafumi Takiguchi

Division of Viral Immunology, Center for AIDS Research, Kumamoto University, Kumamoto, Japan

Phenotypic classification of human CD8+ T cells using three cell surface markers, CD27, CD28 and CD45RA, was recently suggested to be useful for identification of naive, memory and effector CD8+ T cells. However, it still remains unclear whether such classification precisely reflects functional classification of CD8+ T cells. To clarify this, we characterized each CD27CD28CD45RA subset of total and human cytomegalovirus (HCMV)-specific CD8+ T cells by analyzing the expression of perforin and two chemokine receptors, CCR5 and CCR7, as well as their function. An inverse correlation between perforin and CD27 expression was found in all four CD28CD45RA subsets. Therefore, to achieve a phenotypic classification of CD8+ T cells that more precisely reflects their function, the CD27+ subset was divided into $CD27^{low}$ and $CD27^{high}$ subsets based on the expression level of CD27. Functional and flow cytometric analyses of CD27CD28CD45RA subsets showed that this phenotypic classification reflects functional classification of CD8+ T cells. HCMV-specific CD8+ T cells from healthy HCMV-seropositive individuals were predominantly found in effector and memory/effector subsets, indicating that HCMV-specific effector CD8+ T cells are actively induced by HCMV replication in healthy HCMV carriers. Phenotypic analyses of CD8+ T cells using this classification will enable the characterization of antigen-specific CD8+ T cells.

Received	14/8/03
Revised	20/1/04
Accepted	6/2/04

Key words: CTL / Cytomegalovirus / Memory / Effector

1 Introduction

Memory and effector CD8+ T cells play an important role in viral eradication through their ability to produce various factors involved in suppression of viral replication [1–4] as well as in cytolysis of virus-infected cells [5, 6]. Effector cytotoxic CD8+ T cells have the ability to kill target cells through perforin and Fas ligands. CD8+ T cells that can kill target cells can be divided into two groups: effector cells and memory/effector cells. The former express a high level of perforin, have strong cytolytic activity, and produce low levels of cytokines such as IL-2 and IFN-γ, while the latter have medium levels of perforin, cytotoxic activity and produce high levels of cytokines [7, 8]. Memory CD8+ T cells fail to kill target cells but can proliferate and produce cytokines in response to antigen stimulation [7, 9].

[DOI 10.1002/eji.200324478]

Abbreviations: HCMV: Human cytomegalovirus **MFI:** Mean fluorescence intensity **NMFI:** Normalized MFI

Phenotypic classification of memory and effector CD8+ T cells is very useful in many human and animal immunological studies. In humans, previous studies suggested that particular expression patterns of costimulatory receptors CD27 and CD28 as well as CD45RA or CD45RO are associated with the naive, memory and effector function of human CD8+ T cells [8, 10–16]. Effector and memory/effector CD8+ T cells have a $CD28^-CD45RA^+$ or $CD27^-CD45RA^+$ and $CD28^-CD45RA^-$ or $CD27^-CD45RA^-$ phenotype, respectively, while naive and memory CD8+ T cells have a $CD28^+CD45RA^+$ or $CD27^+CD45RA^+$ and $CD28^+CD45RA^-$ or $CD27^+CD45RA^-$ phenotype, respectively [7, 15, 16]. In addition, a recent study of human CD8+ T cells with multi-color flow cytometric analysis showed that $CD27^+CD28^-CD45RA^-CD8^+$ T cells have cytotoxic activity and can effectively produce cytokines, suggesting that this phenotype reflects also memory/effector CD8+ T cells [8]. In another study, human CD8+ T cells were classified into four major subsets according to CD27 and CD28 expression: naive ($CD27^+CD28^+$), early ($CD27^+CD28^+$), intermediate ($CD27^+CD28^-$) and late ($CD27^-CD28^-$), though naive and

early subsets were mostly discriminated by the expression of CD45RA and CCR7 [17].

The chemokine receptor CCR7 is very useful for discriminating naive and memory $CD8^+$ T cells from memory/effector and effector $CD8^+$ T cells [8, 18, 19]. CCR7 functions as a homing receptor and is expressed in naive $CD8^+$ T cells and a subset of memory $CD8^+$ T cells. Previous studies revealed the following classification of $CD8^+$ T cells using CCR7 and CD45RA: naive ($CCR7^+CD45RA^+$), central/memory ($CCR7^+CD45RA^-$) and effector/memory ($CCR7^-CD45RA^{+/-}$) [16, 18, 19]. Recent studies showed that the CCR5 chemokine receptor, whose ligands are RANTES, macrophage inflammatory protein (MIP)-1α and MIP-1β, is expressed in memory, memory/effector and effector $CD8^+$ T cells [8, 20], with the number of $CCR5^+CD8^+$ T cells decreasing during differentiation of $CD27^+CD28^+CD45RA^-$ T cells to $CD27^-CD28^-CD45RA^-$ T cells [20]. These studies imply that these two chemokine receptors are also useful for classification of $CD8^+$ T cells.

A recent study of phenotypic classification using CD27 and CD28 suggested that three phenotypic subsets reflect the functional status of memory and effector $CD8^+$ T cells [17]. However, this study implied that this phenotypic classification of $CD8^+$ T cells is not appropriate because different phenotypic subsets were found in memory $CD8^+$ T cells responding to different viruses. An alternative interpretation of these findings is that this phenotypic classification of $CD8^+$ T cells was incomplete and that memory and effector $CD8^+$ T cells are induced at different stages by different viruses. Previous studies of human $CD8^+$ T cells using these cell surface markers might have only partially classified and analyzed human $CD8^+$ T cells. As these studies did not investigate human $CD8^+$ T cells by both multi-color flow cytometric analysis and functional analysis of each subset, the correlation between the functional subsets and the phenotypic subsets classified by these markers is still unclear.

In the present study, we attempted to classify human $CD8^+$ T cells using three cell surface markers, CD27, CD28, and CD45RA, as well as two ckemokine receptors, CCR5 and CCR7. The function of CD27CD28CD45RA subsets was further investigated to clarify whether our phenotypic classification precisely reflects functional classification. We propose the classification of human $CD8^+$ T cells using quantitative expression of CD27 in addition to qualitative expression of CD28 and CD45RA.

2 Results

2.1 Inverse correlation between perforin and CD27 expression in CD28CD45RA subsets of $CD8^+$ T cells

Perforin is often used as one marker for effector T cells when characterizing $CD8^+$ T cells, because it is a functional molecule for killing cells, which is one of the most important $CD8^+$ T cell functions [5, 7, 15]. To characterize each CD27CD28CD45RA subset of human $CD8^+$ T cells, we stained total $CD8^+$ T cells from eight healthy individuals with mAb specific for CD27, CD28 and CD45RA as well as a perforin-specific mAb, and then analyzed each subset for perforin expression level. First, we analyzed the correlation between perforin and CD27 or CD28 expression. Perforin expression was significantly different between cells expressing a high level of CD27 ($CD27^{high}$) and a low level of CD27 ($CD27^{low}$) ($p<0.005$), while there was no difference in perforin expression between cells expressing high and low levels of CD28 (data not shown). Therefore, we analyzed each CD27CD28CD45RA subset by dividing the $CD27^+$ cells into $CD27^{high}$ and $CD27^{low}$ cells. $CD27^{high}$ cells showed a lower level of perforin than $CD27^{low}$ cells in $CD27^+$ cells of all four CD28CD45RA subsets. Results from a representative individual and all eight healthy individuals are shown in Fig. 1A and B, respectively.

The $CD27^{high}CD28^+CD45RA^-$ subset did not express perforin, while the $CD27^{low/-}CD28^+CD45RA^-$ subsets included a small number of cells expressing a low level of perforin. Perforin expression of the latter subsets was significantly higher than that of the former subset ($p<0.05$; Fig. 1B). Similarly, the $CD27^{high}CD28^+CD45RA^+$ subset did not express perforin, while the $CD27^{low}CD28^+CD45RA^+$ subset included a small number of cells expressing a low level of perforin. The $CD27^{low}CD28^-CD45RA^{+/-}$ subsets contained a large number of cells expressing a low level of perforin, while the $CD27^-CD28^-CD45RA^{+/-}$ subsets included a large number of cells expressing a high level of perforin. In both $CD45RA^+$ and $CD45RA^-$ populations, the $CD27^-CD28^-$ and the $CD27^{low}CD28^-$ subsets expressed significantly higher levels of perforin than the $CD27^{high}CD28^-$ subsets ($CD45RA^+$: $p<0.0005$ and $p<0.001$, respectively; $CD45RA^-$: $p<0.0005$ and $p<0.005$, respectively; Fig. 1B). These results suggest that the $CD27^-CD28^-$ subsets include cytotoxic effector T cells (effector subsets) while the $CD27^{low}CD28^-$ subsets include less differentiated effector T cells (memory/effector T cells).

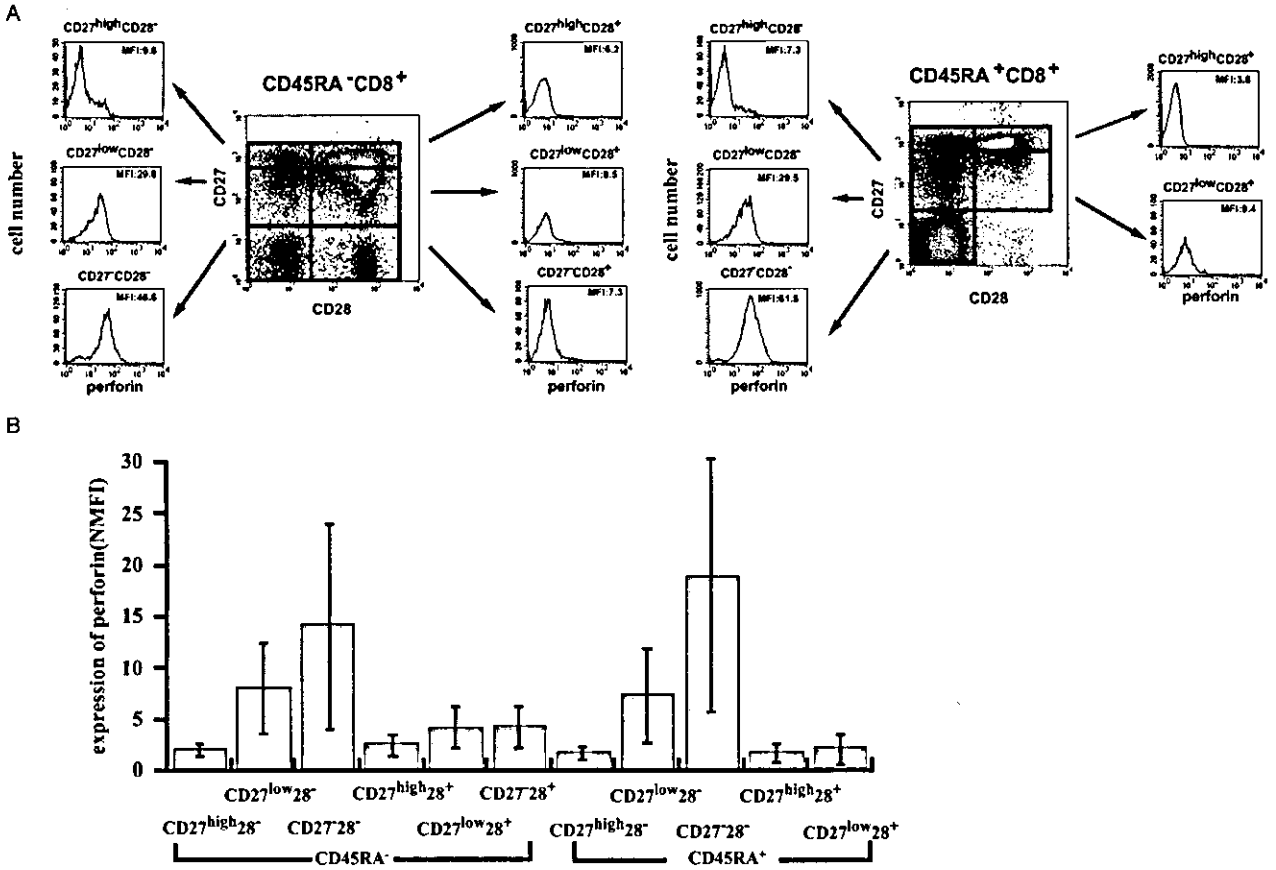

Fig. 1. Perforin expression in different CD27CD28CD45RA subsets of total CD8+ T cells. (A) CD8+ T cells were isolated from individual U13 and then stained with anti-CD27, anti-CD28, anti-CD45RA and anti-perforin mAb. CD45RA+ and CD45RA- T cells were gated and then analyzed for CD27 and CD28 expression. Each population could be separated into five different subsets according to CD27 and CD28 expression ($CD27^{high}CD28^+$, $CD27^{low}CD28^+$, $CD27^{high}CD28^+$, $CD27^{low}CD28^+$, $CD27^-CD28^-$). $CD27^{high}$ and $CD27^{low}$ populations were divided by a quarter of maximum CD27 MFI. In this case, CD27 MFI 495 divided $CD27^{high}$ and $CD27^{low}$ populations because the maximum CD27 MFI is 1,981. The $CD27^-CD28^-$ subset was gated in CD8 T cells stained without antibodies. The CD27CD28CD45RA subsets were gated and then analyzed for perforin expression. Intracellular perforin expression in each CD27CD28CD45RA subset is represented in the upper right of each plot as MFI. (B) Intracellular perforin expression in each CD27CD28CD45RA subset from eight healthy individuals was analyzed. Intracellular perforin expression is represented as NMFI, which is the MFI of cells stained with anti-perforin-PE mAb divided by the MFI of cells stained with the control mouse IgG2b-PE mAb. Mean and standard deviation of NMFI from these eight individuals are shown.

2.2 Correlation between IFN-γ production and perforin expression in CD27CD28CD45RA subsets of CD8+ T cells

The ability of each CD27CD28CD45RA subset to produce IFN-γ was investigated in total CD8+ T cells from three healthy individuals by measuring IFN-γ production after stimulation with anti-CD3 mAb. A significant number of IFN-γ-producing cells were found in seven subsets: $CD27^{low}CD28^-CD45RA^-$, $CD27^-CD28^-CD45RA^-$, $CD27^{low}CD28^-CD45RA^+$, $CD27^-CD28^-CD45RA^+$, $CD27^-CD28^+CD45RA^-$, $CD27^{low}CD28^+CD45RA^-$ and $CD27^{low}CD28^+CD45RA^+$ (Fig. 2A, B). Of these subsets, the $CD27^-CD28^-CD45RA^-$ subset contained the highest number of IFN-γ-producing cells. Three subsets, $CD27^{low}CD28^-CD45RA^{+/-}$ and $CD27^-CD28^-CD45RA^+$, had a higher number of IFN-γ-producing cells than the $CD27^-CD28^+CD45RA^-$ and $CD27^{low}CD28^+CD45RA^{+/-}$ subsets. These results indicate that IFN-γ-producing cells are predominantly found in four subsets ($CD27^-CD28^-CD45RA^{+/-}$ and $CD27^{low}CD28^-CD45RA^{+/-}$) including a higher number of perforin+ cells, though $CD28^-CD45RA^-$ subsets produce much more IFN-γ than $CD28^-CD45RA^+$ subsets.

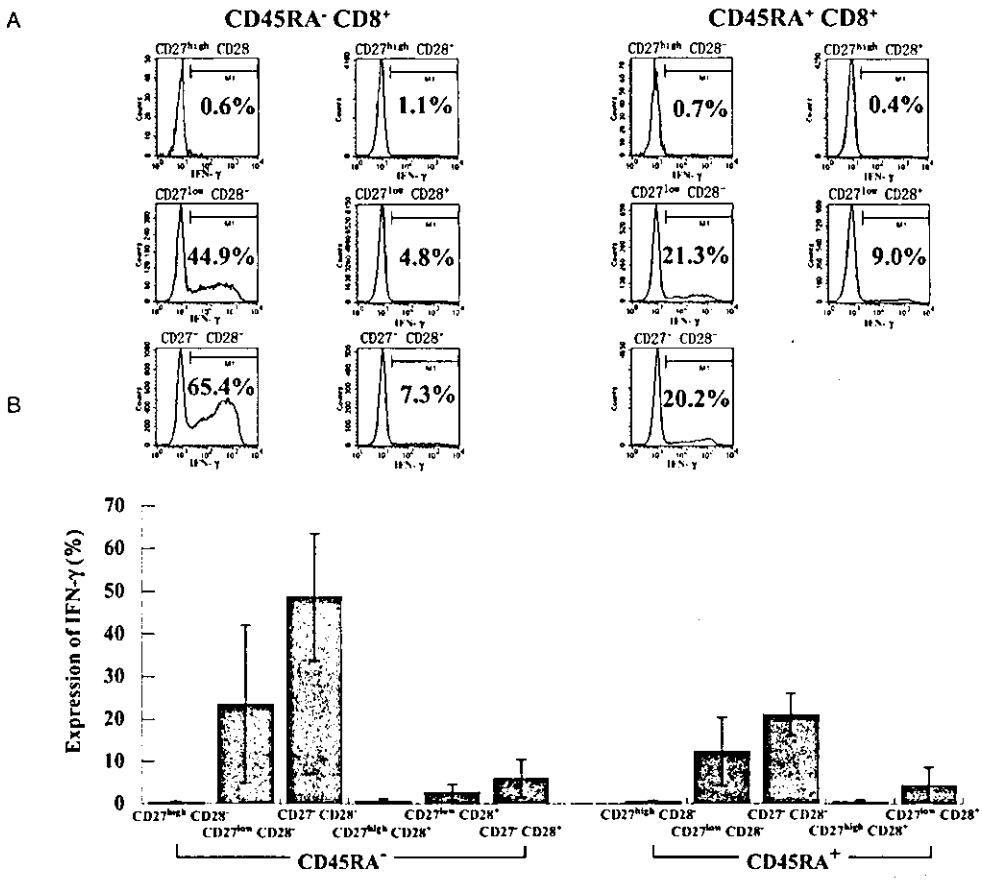

Fig. 2. Anti-CD3 mAb-induced cytokine production by CD8⁺ T cells in different CD27CD28CD45RA subsets. (A) PBMC isolated from healthy individual U4 were cultured in F-bottom 24-well plates coated with or without anti-CD3 mAb (2 μg/ml) in R10 medium for 6 h. IFN-γ-producing cells in different CD27CD28CD45RA subsets of total CD8⁺ T cells were analyzed by flow cytometry. In the absence of anti-CD3 mAb, each subset of total CD8⁺ T cells contained less than 0.6% IFN-γ-producing cells. (B) Mean percentage and standard deviation of IFN-γ-producing cells in different CD27CD28CD45RA subsets of total CD8⁺ T cells from three healthy individuals.

2.3 CCR5 expression decreases during maturation of CD8⁺ T cells

CCR7 is expressed in naive CD8⁺ T cells and central memory CD8⁺ T cells [18, 19]. Recent studies have shown that CCR5 is expressed in memory and effector CD8⁺ T cells and that the number of CCR5⁺ cells decreased during differentiation from the $CD27^-CD28^-CD45RA^-$ subset to the $CD27^+CD28^-CD45RA^-$ subset [8, 21]. These chemokine receptors may be useful to discriminate between naive, memory and effector CD8⁺ T cells. To further investigate CCR5 and CCR7 expression in different CD27CD28CD45RA subsets of total CD8⁺ T cells, we stained total CD8⁺ T cells from seven healthy individuals with anti-CD27, anti-CD28, anti-CD45RA and anti-CCR5 or anti-CCR7 mAb.

Representative results from individual U13 and results from seven healthy individuals are shown in Fig. 3A and B, respectively. CCR7 was expressed on $CD27^{high}CD28^+CD45RA^{+/-}$ subsets, but not on four subsets containing perforin⁺ effector cells ($CD27^{low}CD28^-CD45RA^{+/-}$ and $CD27^-CD28^-CD45RA^{+/-}$). The $CD27^{high}CD28^-CD45RA^+$ subset also included CCR7⁺ cells but not CCR5⁺ cells, suggesting that this subset may have characteristics of naive T cells. The $CD27^{high}CD28^+CD45RA^-$ subset as well as two subsets, $CD27^{low}CD28^+CD45RA^+$ and $CD27^{high}CD28^-CD45RA^-$, included both CCR7⁺ cells and CCR5⁺ cells, although the frequency of these cells varied between these subsets. The $CD27^{low}CD28^+CD45RA^+$ subset included a larger number of CCR7⁺ cells and a smaller number of CCR5⁺ cells than the $CD27^{high}CD28^+CD45RA^-$ memory subset, suggesting that the $CD27^{low}CD28^+CD45RA^+$ subset has characteristics of immature memory T cells rather than the $CD27^{high}CD28^+CD45RA^-$ memory subset. The $CD27^{high}CD28^-CD45RA^-$ subset included a smaller number of CCR7⁺ cells than the $CD27^{high}CD28^+CD45RA^-$

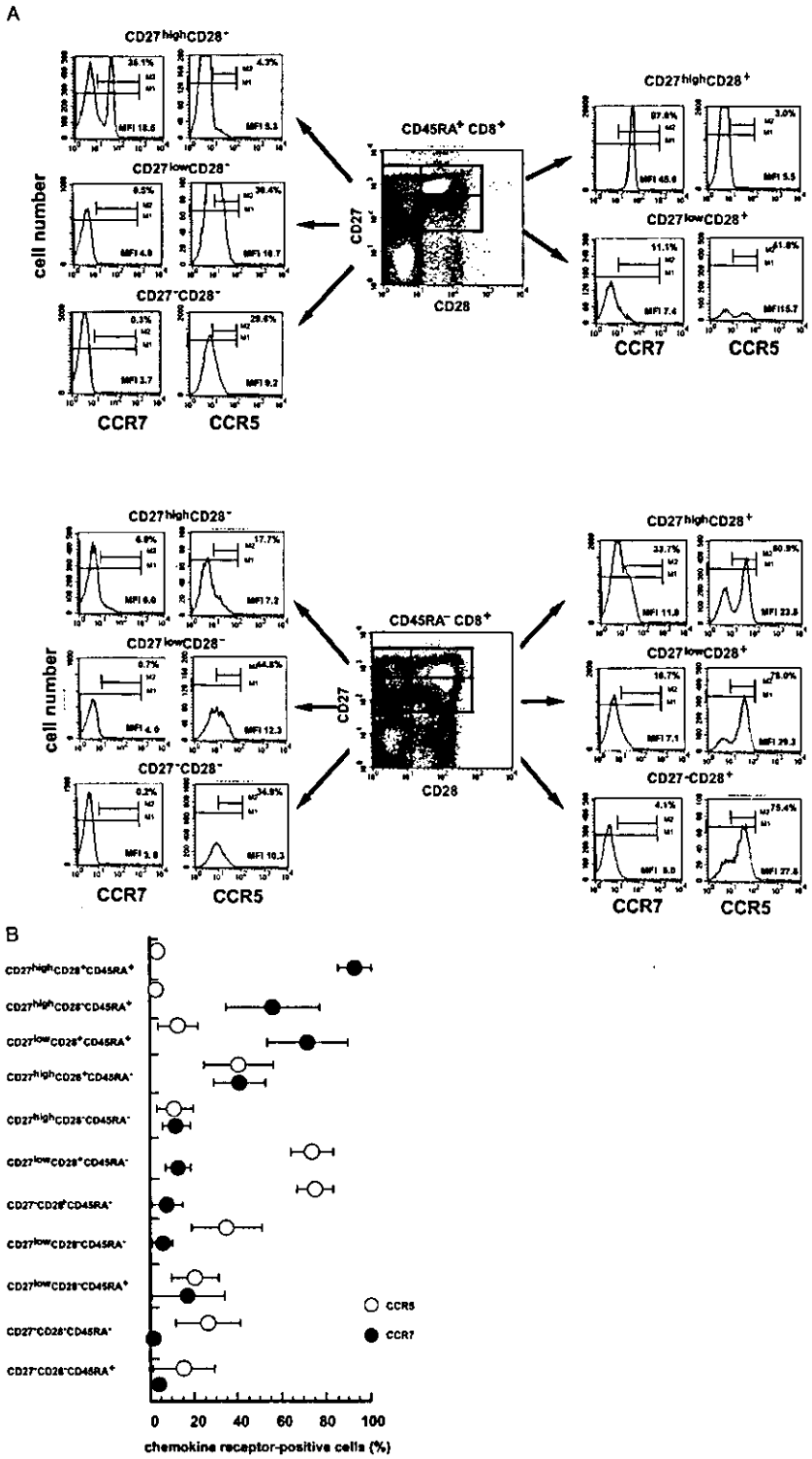

Fig. 3. CCR5 and CCR7 expression on each CD27CD28CD45RA subset of total CD8⁺ T cells. (A) CD8⁺ T cells were isolated from individual U13 and then stained with anti-CD27, anti-CD28, anti-CD45RA and anti-CCR5 or anti-CCR7 mAb. CD45RA⁺ cells were gated and then analyzed for CD27 and CD28 expression. The three CD27CD28 subsets of CD45RA⁻CD8⁺ T cells were further gated for analysis of CCR5 expression. The percentage and MIF of CCR5⁺ or CCR7⁺ cells are shown in the upper right and lower right of each plot, respectively. The MFI for CD8⁺ T cells stained without anti-CCR5 or anti-CCR7 mAb ranged from 3.0 to 3.5. (B) Mean percentage and standard deviation of CCR5⁺ or CCR7⁺ cells in each CD27CD28CD45RA subset from eight healthy individuals.

memory subset, suggesting that the former has characteristics of mature memory T cells rather than the latter.

The $CD27^{low}CD28^{-}CD45RA^{+/-}$ subsets as well as the $CD27^{-}CD28^{-}CD45RA^{+/-}$ subsets expressed CCR5 but not CCR7, though the frequency of $CCR5^{+}$ cells was higher in the $CD27^{low}$ subsets than in the $CD27^{-}$ subsets. The $CD27^{-}$ subsets are thought to be more differentiated effector cells than the $CD27^{low}$ subsets because the former subsets express higher level of perforin than the latter subsets. Thus, these results support the idea that the number of $CCR5^{+}$ cells decreases during maturation to effector T cells. The $CD27^{-}CD28^{+}CD45RA^{-}$ subset also expressed CCR5 but not CCR7, implying that this is an intermediate subset between the $CD27^{low}CD28^{+}CD45RA^{-}$ and $CD27^{-}CD28^{-}CD45RA^{-}$ subsets.

2.4 Human cytomegalovirus-specific $CD8^{+}$ T cells express a memory/effector or effector phenotype

The human cytomegalovirus (HCMV) epitope pp65 495–503 NLVPMVATV (HCMV-1) is an HLA-A*0201-restricted immunodominant epitope [22–24] that is also presented by HLA-A*0206 (our unpublished observation). We generated both HCMV-1-A*0201 and HCMV-1-A*0206 tetramers using this epitope peptide in order to analyze HCMV-specific $CD8^{+}$ T cells from HCMV-seropositive healthy individuals with HLA-A*02 (A*0201 and A*0206). *Ex vivo* flow cytometry analysis using these tetramers demonstrated that approximately 1.0% of total $CD8^{+}$ T cells were $tetramer^{+}$ in 13 of 20 healthy individuals (data not shown). We further analyzed the CD27CD28CD45RA phenotypes of HCMV-specific $CD8^{+}$ T cells. HCMV-specific $CD8^{+}$ T cells showed various phenotypes in eight healthy individuals. They included the $CD27^{-}CD28^{-}CD45RA^{+/-}$ subsets as well as the $CD27^{low}CD28^{+}CD45RA^{-}$ and $CD27^{low}CD28^{-}CD45RA^{+/-}$ subsets (Table 1). The ratio of HCMV-specific $CD8^{+}$ T cells to total $CD8^{+}$ T cells was higher in the $CD27^{low}CD28^{-}CD45RA^{+/-}$ and $CD27^{-}CD28^{-}CD45RA^{+}$ subsets than in other subsets (Table 1), indicating that the relative number of HCMV-specific $CD8^{+}$ T cells increased in these three subsets. This suggests that in healthy individuals, HCMV-specific effector $CD8^{+}$ T cells are always induced from HCMV-specific memory T cells.

We analyzed CCR5 and CCR7 expression in HCMV-specific $CD8^{+}$ T cells by five-color flow cytometry analysis using the HCMV-1-A*0201 tetramer and anti-CD27, anti-CD28, anti-CD45RA and anti-CCR5 or anti-CCR7 mAb (Fig. 4). $CCR7^{+}$ cells were not detected in any subset of HCMV-specific $CD8^{+}$ T cells. The number of $CCR5^{+}$ cells decreased following the same sequence as observed in total $CD8^{+}$ T cells: $CD27^{low}CD28^{+}CD45RA^{-} \rightarrow CD27^{low}CD28^{-}CD45RA^{-} \rightarrow CD27^{-}CD28^{-}CD45RA^{-} \rightarrow CD27^{low}CD28^{-}CD45RA^{+} \rightarrow CD27^{-}CD28^{-}CD45RA^{+}$. This result indicates that the number of $CCR5^{+}$ cells decreases during maturation to effector T cells in HCMV-specific $CD8^{+}$ T cells.

Table 1. Frequency of each CD27CD28CD45RA subset in HCMV-specific and total $CD8^{+}$ T cells from eight healthy individuals

subsets	Percentage of each CD27CD28CD45RA subset in total $CD8^{+}$ T cells (%±SD) [1]	Percentage of each CD27CD28CD45RA subset in $tetramer^{+}$ $CD8^{+}$ T cells (%±SD) [2]	[2]/[1]
$CD27^{high}CD28^{+}CD45RA^{+}$	32.31±19.96	0.63±0.40	0.02±0.02
$CD27^{low}CD28^{+}CD45RA^{+}$	2.77±2.61	0.34±0.29	0.28±0.44
$CD27^{high}CD28^{-}CD45RA^{+}$	1.27±1.22	0.33±0.61	0.49±1.18
$CD27^{low}CD28^{-}CD45RA^{+}$	2.50±1.98	7.27±8.69	3.26±3.02
$CD27^{-}CD28^{-}CD45RA^{+}$	20.20±14.30	21.00±13.76	1.19±0.98
$CD27^{high}CD28^{+}CD45RA^{-}$	5.60±2.97	1.69±1.37	0.41±0.44
$CD27^{low}CD28^{+}CD45RA^{-}$	9.44±6.15	9.59±11.37	1.09±0.83
$CD27^{-}CD28^{+}CD45RA^{-}$	1.40±0.57	1.46±0.70	1.04±0.42
$CD27^{high}CD28^{-}CD45RA^{-}$	0.84±0.49	0.70±0.68	1.08±1.38
$CD27^{low}CD28^{-}CD45RA^{-}$	2.11±0.54	18.64±14.72	9.17±7.02
$CD27^{-}CD28^{-}CD45RA^{-}$	12.58±11.49	28.99±15.03	4.23±5.56

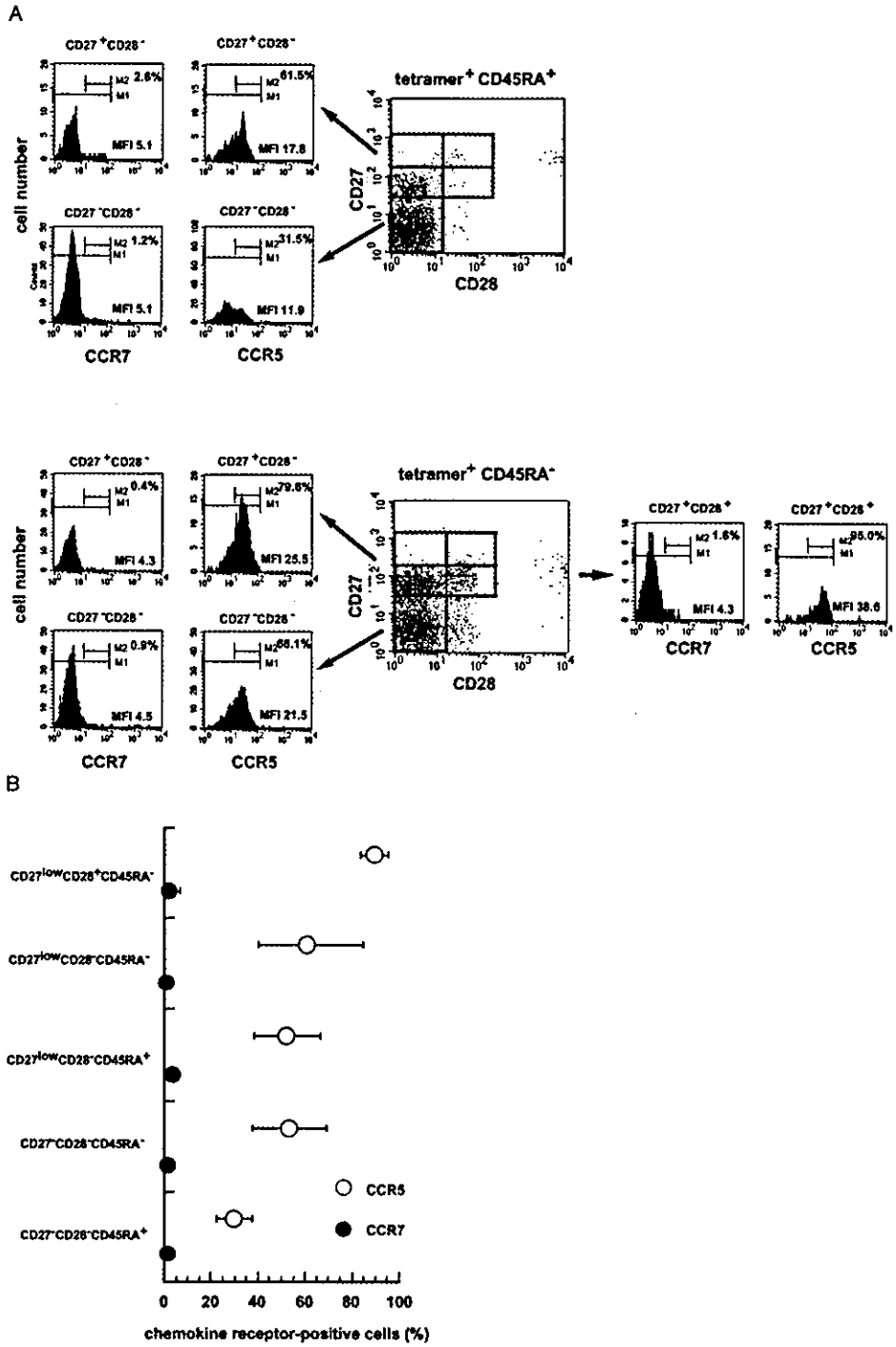

Fig. 4. CCR5 and CCR7 expression on HCMV-1-specific CD45RA⁺CD8⁺ T cells with different CD27CD28 phenotypes. (A) CD8⁺ T cells were isolated from individual U2, and then stained with anti-CD27, anti-CD28, anti-CD45RA and anti-CCR5 or anti-CCR7 mAb as well as HCMV-1-A*0206 tetramer. Tetramer⁺ cells were gated and then analyzed for CD27, CD28 and CD45RA expression. The five CD27CD28CD45RA subsets in which tetramer⁺ cells were found were gated and then analyzed for CCR5 or CCR7 expression. The percentage of CCR5⁺ or CCR7⁺ cells (M2) is shown in the upper right of each plot and the MFI is shown in the lower right. MFI for the five subsets stained without mAb and with mouse IgM mAb (isotype control for anti-CCR7 mAb) ranged from 3.5 to 4.5 and from 3.3 to 4.5, respectively. (B) Mean percentage and standard deviation of CCR5⁺ and CCR7⁺ cells in five CD27CD28CD45RA subsets of tetramer⁺CD8⁺ T cells from three healthy individuals.

2.5 A CD27^{low}CD28$^-$CD45RA$^+$ subset of HCMV-specific CD8$^+$ T cells has cytolytic activity

Although our previous study showed that HCMV-1-specific CD27$^+$CD28$^-$CD45RA$^-$CD8$^+$ T cells have cytotoxic activity against target cells pulsed with HCMV-1 peptide [8], it remains unknown whether the CD27$^{+(low)}$CD28$^-$CD45RA$^+$ subset is able to kill target cells. We first investigated perforin expression of the CD27^{low}CD28$^-$CD45RA$^{+/-}$ and CD27$^-$CD28$^-$CD45RA$^{+/-}$ subsets in HCMV-specific CD8$^+$ T cells using mAb against CD27, CD45RA and perforin as well as the HCMV-1-A*0201 or HCMV-1-A*0206 tetramer. All four CD27CD45RA subsets expressed a high level of perforin though perforin expression in both CD27$^-$CD28$^-$CD45RA$^{+/-}$ subsets was higher than in the CD27^{low}CD28$^-$CD45RA$^{+/-}$ subsets (data not shown). These results suggest that HCMV-specific CD27^{low}CD28$^-$CD45RA$^+$CD8$^+$ T cells also have cytotoxic activity.

We therefore investigated the ability of the CD27^{low}CD28$^-$CD45RA$^+$ subset of HCMV-specific CD8$^+$ T cells to kill target cells. The CD27$^+$CD28$^-$CD45RA$^+$ and CD27$^-$CD28$^-$CD45RA$^+$ subsets of total CD8$^+$ T cells from individuals M20 and U9 were sorted (Fig. 5A), and then their cytolytic activity for HLA-A*0201$^+$ target cells pulsed with HCMV-1 peptide was examined at various tetramer$^+$CD8$^+$ T cell to target ratios. Cells from both

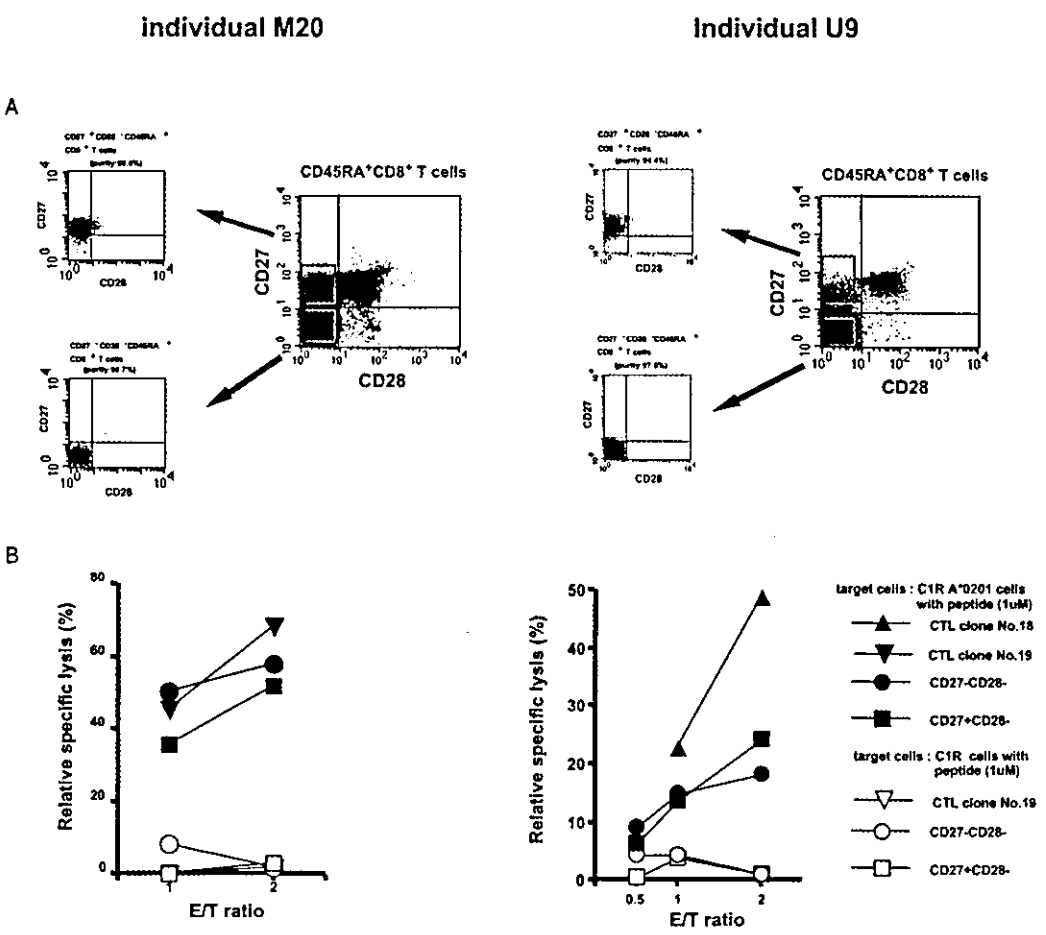

Fig. 5. Cytotoxic activity of CD27$^+$ and CD27$^-$ populations of HCMV-specific CD28$^-$CD45RA$^+$CD8$^+$ T cells. (A) Isolation of CD27$^+$CD28$^-$ and CD27$^-$CD28$^-$ subsets of total CD45RA$^+$CD8$^+$ T cells. CD8$^+$ T cells were isolated from individuals M20 and U9 using MACS. CD27$^+$CD28$^-$CD45RA$^+$CD8$^+$ and CD27$^-$CD28$^-$CD45RA$^+$CD8$^+$ T cells were then isolated from the CD8$^+$ T cells using a cell sorter. The percentage of HLA-A*0201-restricted, HCMV-1-specific CD8$^+$ T cells in each subset was measured using HCMV-1-A*0201 tetramer. (B) Cytotoxic activity of two CD27CD28 subsets of HCMV-specific CD45RA$^+$CD8$^+$ T cells. The relative cytotoxic activity of the CD27$^-$CD28$^-$ (filled circles) and CD27$^+$CD28$^-$ (filled squares) subsets as well as HCMV-1-specific CTL clones (filled triangles) for C1R-A*0201 cells pulsed with HCMV-1 peptide was measured at different effector (tetramer$^+$ cells) to target ratios. The relative cytotoxic activity of CD27$^-$CD28$^-$ (empty circles) and CD27$^+$CD28$^-$ (empty squares) subsets as well as CTL clones (empty triangles) for C1R cells pulsed with HCMV-1 peptides was also measured at different effector (tetramer$^+$ cells) to target ratios.

subsets effectively killed target cells pulsed with the HCMV-1 peptide (Fig. 5B). Since HCMV-1-specific CD8+ T cells in the $CD27^+CD28^-CD45RA^+$ subset showed a $CD27^{low}CD28^-CD45RA^+$ phenotype in these individuals (Table 1), these results together indicate that HCMV-1-specific $CD27^{low}CD28^-CD45RA^+CD8^+$ T cells have cytotoxic activity. Thus, the present study together with a previous study [8] showed that both $CD27^{low}CD28^-CD45RA^+$ and $CD27^{low}CD28^-CD45RA^-$ subsets of HCMV-1-specific CD8+ T cells have cytotoxic activity.

3 Discussion

Recent studies demonstrated that perforin+CD8+ T cells express a $CD27^-$ phenotype [17, 25]. The present study confirmed these studies and further showed an inverse correlation between perforin and CD27 expression. The $CD27^{low}CD28^-CD45RA^{+/-}$ and $CD27^-CD28^-CD45RA^{+/-}$ subsets showed cytolytic activity and expressed significantly higher levels of perforin than other subsets, indicating that these subsets are mostly cytotoxic effector T cells. The former subsets may have characteristics of immature effector T cells (memory/effector T cells) since the $CD27^{low}CD28^-CD45RA^{+/-}$ subsets expressed lower levels of perforin than the $CD27^-CD28^-CD45RA^{+/-}$ subsets. Thus, we here showed that CD8+ T cells with cytotoxic effector function could be effectively discriminated from other CD8+ T cells by this classification using CD28, CD45RA and quantitative expression of CD27.

It is hardly possible to discriminate naive CD8+ T cells from memory CD8+ T cells by perforin expression because both CD8+ T cells do not express perforin. On the other hand, two chemokine receptors, CCR7 and CCR5, are useful to discriminate between naive, memory and effector CD8+ T cells, because CCR7 and CCR5 are expressed in naive CD8+ T cells and central memory CD8+ T cells [18, 19] and in memory CD8+ T cells and a part of effector CD8+ T cells [21], respectively. A previous study showed that EBV-specific CD8+ T cells expressed $CD27^+CD28^+CD45RA^-$ phenotype (both $CD27^{high}CD28^+CD45RA^-$ and $CD27^{low}CD28^+CD45RA^-$) as well as both CCR7 and CCR5, whereas they failed to kill target cells ([8], our unpublished observation), suggesting that the $CD27^+CD28^+CD45RA^-$ subset is a memory CD8+ T cell subset. However, the $CD27^{low}CD28^+CD45RA^-$ subset included a larger number of cells expressing a low level of perforin than the $CD27^{high}CD28^+CD45RA^-$ subset. In addition, the former subset included a large number of $CCR5^+CCR7^-$ cells while the latter included both $CCR5^+$ cells and $CCR7^+$ cells. These findings indicate that the $CD27^{low}CD28^+CD45RA^-$ subset is a more differentiated memory subset than the $CD27^{high}CD28^+CD45RA^-$ subset.

The $CD27^{high}CD28^+CD45RA^+$ subset included a large number of $CCR7^+CCR5^-$ cells while the $CD27^{low}CD28^+CD45RA^+$ and $CD27^{high}CD28^+CD45RA^-$ subsets included both $CCR5^+$ cells and $CCR7^+$ cells. The $CD27^{high}CD28^+CD45RA^+$ subset had a higher number of $CCR7^+$ cells than the $CD27^{low}CD28^+CD45RA^-$ subset, implying that the latter subset represents more mature T cells than the former. Thus, these four subsets can be thought of as follows. The $CD27^{high}CD28^+CD45RA^+$ subset mostly includes naive T cells. The $CD27^{low}CD28^+CD45RA^+$ subset might include both naive cells and memory T cells. The $CD27^{high}CD28^+CD45RA^-$ memory subset mostly includes undifferentiated memory T cells, while the $CD27^{low}CD28^+CD45RA^-$ memory subset includes differentiated memory T cells.

The $CD27^{high}CD28^-CD45RA^{+/-}$ subsets mostly included cells not expressing perforin, suggesting that these subsets are naive or memory T cells. The $CD27^{high}CD28^-CD45RA^+$ subset included a large number of $CCR7^+CCR5^-$ cells and showed much weaker proliferation ability than memory, memory/effector and effector subsets (data not shown), while the $CD27^{high}CD28^-CD45RA^-$ subset included a small number of $CCR7^+$ cells and $CCR5^+$ cells. These findings imply that these subsets carry intermediate characteristics between memory and naive subsets though the $CD27^{high}CD28^-CD45RA^-$ subset has more mature characteristics than the $CD27^{high}CD28^-CD45RA^+$ subset.

A recent study of $CD45RA^-$ subset showed that the percentage of $CCR5^+$ cells was the highest in the $CD27^+CD28^+CD45RA^-$ memory CD8+ T cell subset, and decreased during the following differentiation sequence: $CD27^+CD28^+CD45RA^- \rightarrow CD27^+CD28^-CD45RA^- \rightarrow CD27^-CD28^-CD45RA^-$ [8]. The present study analyzed all CD27CD28CD45RA subsets and further demonstrated that the percentage of $CCR5^+$ cells decreased according to the following sequence: $CD27^{high}CD28^+CD45RA^-$ and $CD27^{low}CD28^+CD45RA^- \rightarrow CD27^{low}CD28^-CD45RA^{+/-} \rightarrow CD27^-CD28^-CD45RA^{+/-}$, supporting that CCR5 expression decreases during differentiation from memory CD8+ T cells to effector CD8+ T cells. As CCR5 functions as a chemokine receptor for RANTES and MIP-1β [20], this receptor may play an important role in migration of memory and memory/effector CD8+ T cells to inflammation sites. Indeed, our previous study showed effective migration of memory and effector subsets in response to RANTES [21].

IFN-γ-producing cells were predominantly found in effector and memory/effector subsets, while a very small number of IFN-γ-producing cells were found in memory subsets. A previous study showed that memory CD8+ T cells can produce IFN-γ [7]. This difference may result

from different experimental conditions: in the present study, the $CD8^+$ T cells were stimulated with anti-CD3 mAb, whereas they were stimulated with PMA and ionomycin or with PMA and anti-CD3 mAb in a previous study. Interestingly, our data showed that the number of cytokine-producing cells in the $CD27^{low/-}CD28^-CD45RA^+$ subset was much lower than that in the $CD27^{low/-}CD28^-CD45RA^-$ subset. This indicates that IFN-γ production does not exactly correlate with perforin expression. Further analysis of production of other cytokines is required to characterize these CD27CD28CD45RA subsets.

Most EBV-specific $CD8^+$ T cells have a $CD27^+CD28^+CD45RA^-$ memory phenotype [8, 17, 26, 27], while HCMV-specific $CD8^+$ T cells express various phenotypes, from memory to effector phenotype [12, 17, 24]. Here we show that HCMV-specific $CD8^+$ T cells are at various differentiation stages, but predominantly express four effector and memory/effector phenotypes (Table 1). In addition, we show that these HCMV-specific $CD8^+$ T cells had cytolytic activity. These observations indicate that HCMV-specific $CD8^+$ T cells have effector function in healthy individuals. The $CD27^{low}CD28^-CD45RA^+$, $CD27^{low}CD28^-CD45RA^-$ and $CD27^-CD28^-CD45RA^-$ subsets relatively increased in HCMV-specific $CD8^+$ T cells, implying that HCMV actively replicates and induces HCMV-specific effector $CD8^+$ T cells from memory $CD8^+$ T cells in healthy individuals.

In the present study, we show an inverse correlation between perforin and CD27 expression. Human $CD8^+$ T cells were classified based on quantitative expression of CD27 in addition to qualitative expression of CD28 and CD45RA. This phenotypic classification enabled a more precise reflection of the function of $CD8^+$ T cells than previous phenotypic classification using qualitative expression of these three markers. According to this classification, HCMV-specific $CD8^+$ T cells observed in healthy individuals were identified as effector and memory/effector T cells. Further characterization of these subsets will contribute to the studies concerning the role of $CD8^+$ T cells in patients with various diseases.

4 Materials and methods

4.1 Blood samples

Blood samples were taken from healthy, HCMV-seropositive adult individuals with HLA-A*02 (A*0201 and A*0206).

4.2 Peptides

The HLA-A*0201-restricted HCMV-specific CTL epitope, pp65 495–503 NLVPMVATV (HCMV-1), was previously identified [22]. This peptide was generated using an automated peptide synthesizer with 9-fluorenylmethoxycarbonyl (Fmoc) strategy followed by cleavage. The purity of the synthesized peptide was examined by HPLC and mass spectrometry.

4.3 Cells

C1R cells expressing HLA-A*0201 (C1R-A*0201) were previously generated [28], and were maintained in RPMI 1640 medium supplemented with 10% FCS and 0.15 mg/ml hygromycin B. Two HLA-A*02-restricted, HCMV-1-specific CTL clones were recently established, and were maintained in RPMI 1640 medium supplemented with 10% FCS and 200 IU/ml r-human IL-2.

4.4 Monoclonal antibodies

Anti-CD27-FITC, anti-CD28-FITC, anti-CD28-PE, anti-CD28-Cy-Chrome, anti-CD28-APC, anti-CD45RA-Cy-Chrome, anti-CCR5-FITC, anti-CCR7 and anti-perforin-FITC mAb were obtained from Pharmingen International (San Diego, CA). Anti-CD45RA-ECD was obtained from Immunotech (Marseille, France). Anti-CD8-FITC, anti-CD8-APC and anti-IFN-γ-FITC mAb were obtained from Dako A/S (Glostrup, Denmark).

4.5 HLA class I-HCMV-1 peptide tetramers

HLA class I-peptide tetrameric complexes were synthesized as previously described [29]. The HCMV CTL epitope (HCMV-1) was used for refolding of HLA class I molecules. The HLA class I-peptide complexes were refolded *in vitro* and the resulting 45-kDa complexes were isolated using gel filtration on a Superdex G75 column (Amersham Pharmacia Biotech, Little Chalfont, GB). Purified complexes were biotinylated using BirA enzyme (Avidity, Denver, CO). The biotinylated complexes were purified using gel filtration first on a Superdex G75 column and then on a MonoQ column (Amersham Pharmacia Biotech). HLA class I-peptide tetrameric complexes (HCMV-1-A*0201 and HCMV-1-A*0206 tetramers) were mixed with APC-labeled streptavidin (Molecular Probes, Inc., Eugene, OR) or APC-Cy7-labeled streptavidin (Caltag Laboratories, Burlingame, CA) at a molar ratio of 4:1.

4.6 Flow cytometric analysis

$CD8^+$ T cells were purified from cryopreserved or fresh PBMC using anti-CD8-coated magnetic beads (MACS CD8 Microbeads; Miltenyi Biotec, Bergisch Gladbach, Germany).

The percentage of $CD8^+$ T cells in purified cells was >98%. $CD8^+$ T cells (1×10^6) were mixed with HCMV-1-A*0201 or HCMV-1-A*0206 tetramer at a concentration of 0.02–0.04 mg/ml. After incubation at 37°C for 30 min, the cells were washed once with RPMI/10% FCS, and then anti-CD27, anti-CD28, anti-CD45RA, anti-CCR5 or anti-CCR7 mAb was added to the cell suspension. The cells were incubated at 4°C for 30 min, and then the cells were washed two times with PBS/10% FCS.

To determine intracellular perforin expression in CD27CD28CD45RA subsets of both tetramer+ cells and total $CD8^+$ T cells, cells stained with anti-CD27, anti-CD28 and anti-CD45RA mAb were fixed with 4% paraformaldehyde at 4°C for 20 min, then permeabilized with PBS supplemented with 0.1% saponin containing 20% FCS (permeabilizing buffer) at 4°C for 10 min. Cells were washed with permeabilizing buffer and then resuspended in 100 µl of the same buffer. Anti-perforin mAb was added, the cell suspension was incubated at 4°C for 30 min, and the cells were then washed three times in permeabilizing buffer at 4°C. PE-labeled mouse IgG1 was used as negative control.

The cells were finally resuspended in PBS containing 2% paraformaldehyde, and then analyzed using a FACSCalibur or FACSVantage SE with Cell Quest software (Becton Dickinson, San Jose, CA). Between 70,000 and 200,000 gated events were acquired for analysis of intracellular perforin. Intracellular perforin expression is represented as the normalized mean fluorescence intensity (NMFI), which is the mean fluorescence intensity (MFI) of cells stained with anti-perforin-PE mAb divided by the MFI of cells stained with the control mouse IgG1-PE mAb. Statistical analysis of perforin expression was performed with Statview 4.02 (Abacus Concepts, Berkeley, CA) using Mann-Whitney's U-test.

4.7 Assay for cytotoxic activity

Cytotoxic activity was measured by a standard ^{51}Cr-release assay as follows. Target cells (2×10^5) were incubated for 60 min with 100 µCi $Na_2{}^{51}Cr$ in saline and then washed three times with RPMI 1640 medium containing 10% NCS. Labeled target cells (2×10^3/well) were added into U-bottom 96-well plates with various amounts of peptide. After incubation for 1 h, $CD8^+$ T cells purified by anti-CD8 mAb-coated beads or $CD27^-CD28^-CD45RA^+CD8^+$ and $CD27^+CD28^-CD45RA^+CD8^+$ T cells purified by a cell sorter (FACSVantage SE) were added and the mixtures were incubated for 6 h at 37°C. The supernatants were then collected and analyzed with a gamma counter.

4.8 Measurement of cytokine-producing cells by flow cytometry

To measure cytokine production in CD27CD28CD45RA subsets of total $CD8^+$ T cells, $CD8^+$ T cells were purified from fresh PBMC from healthy individuals using anti-CD8-coated magnetic beads (MACS CD8 Microbeads). $CD8^+$ T cells were cultured in F-bottom 24-well plates coated with or without anti-CD3 mAb (2 µg/ml) in R10 medium for 6 h. After the first 2 h of incubation, brefeldin A (10 µg/ml) was added to each well. The cells were then stained with a mixture of anti-CD27, anti-CD28 and anti-CD45RA mAb, fixed with 4% paraformaldehyde at 4°C for 20 min, and then permeabilized with PBS supplemented with 0.1% saponin containing 20% NCS (permeabilizing buffer) at 4°C for 10 min. Cells were resuspended in permeabilizing buffer and then stained with anti-IFN-γ mAb. The cells were finally resuspended in PBS containing 2% paraformaldehyde and then the percentage of intracellular IFN-γ^+ cells was analyzed by flow cytometry.

Acknowledgements: This research was supported by a Grant-in-Aid for Scientific Research from the Ministry of Education, Science, Sport and Culture, the Government of Japan and a grant from Japan Health Science Foundation. The authors thank Sachiko Sakai for secretarial assistance.

References

1 **Guidotti, L. G. and Chisari, F. V.,** To kill or to cure: options in host defense against viral infection. *Curr. Opin. Immunol.* 1996. **8:** 478–483.

2 **Cocchi, F., DeVico, A. L., Garzino-Demo, A., Arya, S. K., Gallo, R. C. and Lusso, P.,** Identification of RANTES, MIP-1α, and MIP-1β as the major HIV-suppressive factors produced by $CD8^+$ T cells. *Science* 1995. **270:** 1811–1815.

3 **Levy, J. A., Mackewicz, C. E. and Barker, E.,** Controlling HIV pathogenesis: the role of the noncytotoxic anti-HIV response of $CD8^+$ T cells. *Immunol. Today* 1996. **17:** 217–224.

4 **Yang, O. O., Kalams, S. A., Trocha, A., Cao, H., Luster, A., Johnson, R. P. and Walker, B. D.,** Suppression of human immunodeficiency virus type 1 replication by $CD8^+$ cells: evidence for HLA class I-restricted triggering of cytolytic and noncytolytic mechanisms. *J. Virol.* 1997. **71:** 3120–3128.

5 **Liu, C. C., Walsh, C. M. and Young, J. D.,** Perforin: structure and function. *Immunol. Today* 1995. **16:** 194–201.

6 **Trapani, J. A., Sutton, V. R. and Smyth, M. J.,** CTL granule: evolution of vesicles essential for combating virus infections. *Immunol. Today* 1999. **20:** 351–356.

7 **Hamann, D., Baars, P. A., Rep, M. H., Hooibrink, B., Kerkhof-Garde, S. R., Klein, M. R. and van Lier, R. A.,** Phenotypic and functional separation of memory and effector human $CD8^+$ T cells. *J. Exp. Med.* 1997. **186:** 1407–1418.

8 **Tomiyama, H., Matsuda, T. and Takiguchi, M.,** Differentiation of human $CD8^+$ T cells from a memory to memory/effector phenotype. *J. Immunol.* 2002. **168:** 5538–5550.

9 **Kaech, S., Hemby, M. S., Kersh, E. and Ahmed, R.,** Molecular and functional profiling of memory CD8 T cell differentiation. *Cell* 2002. **111:** 837–851.

10 **Posnett, D. N., Edinger, J. W., Manavalan, J. S., Irwin, C. and Marodon, G.,** Differentiation of human CD8 T cells: implications for *in vivo* persistence of $CD8^+CD28^-$ cytotoxic effector clones. *Int. Immunol.* 1999. **11:** 229–241.

11 **Nociari, M. M., Telford, W. and Russo, C.,** Postthymic development of $CD28^-CD8^+$ T cell subset: age-associated expansion and shift from memory to naive phenotype. *J. Immunol.* 1999. **162:** 3327–3335.

12 **Kern, F., Khatamzas, E., Surel, I., Frommel, C., Reinke, P., Waldrop, S. L., Picker, L. J. and Volk, H. D.,** Distribution of human CMV-specific memory T cells among the $CD8^{pos}$. subset defined by CD57, CD27, and CD45 isoforms. *Eur. J. Immunol.* 1999. **29:** 2908–2915.

13 **Wills, M. R., Carmichael, A. J., Weekes, M. P., Mynard, K., Okecha, G., Hicks, R. and Sissons, J. G.,** Human virus-specific $CD8^+$ CTL clones revert from $CD45RO^{high}$ to $CD45RA^{high}$ *in vivo*: $CD45RA^{high}$ $CD8^+$ T cells comprise both naive and memory cells. *J. Immunol.* 1999. **165:** 7080–7087.

14 **Weekes, M. P., Carmichael, A. J., Wills, M. R., Mynard, K. and Sissons, J. G.,** Human $CD28^-CD8^+$ T cells contain greatly expanded functional virus-specific memory CTL clones. *J. Immunol.* 1999. **162:** 7569–7577.

15 **Hamann, D., Roos, M. T. and van Lier, R. A.,** Faces and phases of human $CD8^+$ T cell development. *Immunol. Today* 1999. **20:** 177–180.

16 **Sobao, Y., Tomiyama, H., Nakamura, S., Sekihara, H., Tanaka, K. and Takiguchi, M.,** Visual demonstration of hepatitis C virus-specific memory $CD8^+$ T cell expansion in patients with acute hepatitis C. *Hepatology* 2001. **33:** 287–294.

17 **Appay, V., Dunbar, P. R., Callan, M., Klenerman, P., Gillespie, G. M., Papagno, L., Ogg, G. S., King, A., Lechner, F., Spina, C. A., Little, S., Havlir, D. V., Richman, D. D., Gruener, N., Page, G., Waters, A., Easterbrool, P., Salio, M., Cerundolo, V., McMichael, A. J. and Rowland-Jones, S. L.,** Memory $CD8^+$ T cells vary in differentiation phenotype in different persistent virus infections. *Nat. Med.* 2002. **8:** 379–385.

18 **Sallusto, F., Lenig, D., Forster, R., Lipp, M. and Lanzavecchia, A.,** Two subsets of memory T lymphocytes with distinct homing potentials and effector functions. *Nature* 1999. **401:** 708–712.

19 **Champagne, P., Ogg, G. S., King, A. S., Knabenhans, C., Ellefsen, K., Nobile, M., Appay, V., Rizzardi, G. P., Fleury, S., Lipp, M., Förster, R., Rowland-Jones, S., Sékaly, R. P., McMichael, A. J. and Pantaleo, G.,** Skewed maturation of memory HIV-specific CD8 T lymphocytes. *Nature* 2001. **410:** 106–111.

20 **Sallusto, F., Mackay, C. R. and Lanzavacchia, A.,** The role of chemokine receptors in primary, effector, and memory immune responses. *Annu. Rev. Immunol.* 2000. **18:** 593–620.

21 **Fukada, K., Sobao, Y., Tomiyama, H., Oka, S. and Takiguchi, M.,** Functional expression of the chemokine receptor CCR5 on virus epitope-specific memory and effector $CD8^+$ T cells. *J. Immunol.* 2002. **168:** 2225–2232.

22 **Wills, M. R., Carmichael, A. J., Mynard, K., Jin, X., Weekes, M. P., Plachter, B. and Sissons, J. G.,** The human cytotoxic T-lymphocyte (CTL) response to cytomegalovirus is dominated by structural protein pp65: frequency, specificity, and T cell receptor usage of pp65-specific CTL. *J. Virol.* 1996. **70:** 7569–7579.

23 **Gillespie, G. M., Wills, M. R., Appay, V., O'Callaghan, C., Murphy, M., Smith, N., Sissons, P., Rowland-Jones, S., Bell, J. I. and Moss, P. A.,** Functional heterogeneity and high frequencies of cytomegalovirus-specific $CD8^+$ T lymphocytes in healthy seropositive donors. *J. Virol.* 2000. **74:** 8140–8150.

24 **Reddehase, M. J.,** The immunogenicity of human and murine cytomegaloviruses. *Curr. Opin. Immunol.* 2000. **12:** 390–396.

25 **Campbell, J. J., Murphy, K. E. and Kunkel, E. J.,** CCR7 expression and memory T cell diversity in humans. *J. Immunol.* 2001. **166:** 877–884.

26 **Tan, L. C., Gudgeon, N., Annels, N. E., Hansasuta, P., O'Callaghan, C. A., Rowland-Jones, S., McMichael, A. J., Rickinson, A. B. and Callan, M. F.,** A re-evaluation of the frequency of $CD8^+$ T cells specific for EBV in healthy virus carriers. *J. Immunol.* 1999. **162:** 1827–1835.

27 **Hislop, A. D., Gudgeon, N. H., Callan, M. F., Fazou, C., Hasegawa, H., Salmon, M. and Rickinson, A. B.,** EBV-specific $CD8^+$ T cell memory: relationships between epitope specificity, cell phenotype, and immediate effector function. *J. Immunol.* 2001. **167:** 2019–2029.

28 **Karaki, S., Kariyone, A., Kato, N., Kano, K., Iwakura, Y. and Takiguchi, M.,** HLA-B51 transgenic mice as recipients for production of polymorphic HLA-A, B-specific antibodies. *Immunogenetics* 1993. **37:** 139–142.

29 **Altman, J. D., Moss, P. A., Goulder, P. J., Barouch, D. H., McHeyzer-Williams, M. G., Bell, J. I., McMichael, A. J. and Davis, M. M.,** Phenotypic analysis of antigen-specific T lymphocytes. *Science* 1996. **274:** 94–96.

Correspondence: Masafumi Takiguchi, Division of Viral Immunology, Center for AIDS Research, Kumamoto University, 2-2-1 Honjo, Kumamoto 860-0811, Japan
Fax: +81-96-373-6532
e-mail: masafumi@kaiju.medic.kumamoto-u.ac.jp

Cutting Edge: Expression of Chemokine Receptor CXCR1 on Human Effector CD8$^+$ T Cells[1]

Hiroshi Takata, Hiroko Tomiyama, Mamoru Fujiwara, Naoki Kobayashi, and Masafumi Takiguchi[2]

IL-8 is a potent inflammatory cytokine that induces chemotaxis of neutrophils expressing CXCR1 and CXCR2, thus indicating its involvement in the migration of these cells to inflammatory sites where bacteria proliferate. Presently, we showed that CXCR1$^+$ cells were predominantly found among CD8$^+$ T cells having effector phenotype, and that the expression of CXCR1 was positively correlated with that of perforin, suggesting that CXCR1 is expressed on effector CD8$^+$ T cells. Indeed, human CMV-specific CD8$^+$ T cells from healthy individuals, which mostly express the effector phenotype and have cytolytic function, expressed CXCR1, whereas EBV-specific CD8$^+$ T cells, which mostly express the memory phenotype and have no cytolytic function, did not express this receptor. The results of a chemotaxis assay showed that the migration of CXCR1$^+$CD8$^+$ T cells was induced by IL-8. These results suggest that the IL-8-CXCR1 pathway plays an important role in the homing of effector CD8$^+$ T cells. The Journal of Immunology, 2004, 173: 2231–2235.

Memory and effector CD8$^+$ T cells play an important role in the eradication of viruses and tumor cells through their ability to produce various factors involved in the suppression of viral replication (1, 2) and to cause cytolysis of virus-infected and tumor cells (3). Effector CD8$^+$ T cells have the ability to kill target cells through the action of perforin and Fas ligands. These cells express a high level of perforin and produce cytokines such as TNF-α and IFN-γ (4). Previous studies suggested that particular expression patterns of costimulatory receptors CD27 and CD28 as well as CD45RA or CD45RO are associated with the naive, memory, and effector functions of human CD8$^+$ T cells (5–8). Multicolor flow cytometric analysis demonstrated that effector and memory/effector CD8$^+$ T cells, both of which have cytolytic activity, have the phenotypes of CD27$^-$CD28$^-$CD45RA$^{+/-}$ and CD27^{low}CD28$^-$CD45RA$^{+/-}$, respectively (4).

The chemokine receptor CCR7 is useful for discriminating naive and central memory CD8$^+$ T cells from memory/effector and effector CD8$^+$ T cells (9). CCR7 functions as a homing receptor and is expressed on naive CD8$^+$ T cells and on a subset of memory CD8$^+$ T cells. A previous study resulted in the following classification of CD8$^+$ T cells based on CCR7 and CD45RA: naive, CCR7$^+$CD45RA$^+$; central memory, CCR7$^+$CD45RA$^-$; and effector/memory, CCR7$^-$CD45RA$^{+/-}$ (9). A recent study showed that the CCR5 chemokine receptor is expressed on memory, memory/effector, and effector CD8$^+$ T cells, with the number of CCR5$^+$CD8$^+$ T cells decreasing during the differentiation of CD27$^+$CD28$^+$CD45RA$^-$ memory T cells into CD27$^-$CD28$^-$CD45RA$^{+/-}$ effector T cells (5). These findings imply that these two chemokine receptors are also useful for the classification of CD8$^+$ T cells.

Two IL-8 receptors, CXCR1 and CXCR2, are expressed on the surface of neutrophils, monocytes, mast cells, NK cells, and eosinophils (10–12). IL-8 can attract these cells (11), indicating that these IL-8 receptors play an important role in the migration of these cells to sites of inflammation. Thus, the cells expressing these IL-8 receptors are involved in innate immunity. Concerning the cells involved in acquired immunity, such as CD8$^+$ and CD4$^+$ T cells, a previous study showed that some CD8$^+$ T cells express these receptors (13). However, there has been no detailed analysis regarding the expression of these receptors on CD8$^+$ T cells.

In the present study, we investigated the expression and function of CXCR1 on human CD8$^+$ T cells. The results showed that CXCR1 was expressed on effector CD8$^+$ T cells and that the migration of CXCR1$^+$CD8$^+$ T cells was induced by IL-8. Our present data have thus revealed an important role played by CXCR1 in acquired immunity.

Materials and Methods

Antibodies

Anti-CD27-FITC, anti-CXCR1-FITC (5A12), anti-CD28-allophycocyanin, and anti-perforin-FITC mAbs were obtained from BD Pharmingen (San Diego, CA). Anti-CD45RA-ECD was purchased from Immunotech (Marseille, France). Anti-CD3-FITC, anti-CD8-allophycocyanin, anti-CXCR1-PE (42705.111), and anti-CXCR2-PE (48311.211) mAbs were obtained from DakoCytomation (Glostrup, Denmark). Human IgG came from Sigma-Aldrich (St. Louis, MO).

Division of Viral Immunology, Center for AIDS Research, Kumamoto University, Honjo, Kumamoto, Japan

Received for publication March 23, 2004. Accepted for publication June 22, 2004.

The costs of publication of this article were defrayed in part by the payment of page charges. This article must therefore be hereby marked *advertisement* in accordance with 18 U.S.C. Section 1734 solely to indicate this fact.

[1] This work was supported by a grant-in-aid for scientific research from the Ministry of Health, Labor and Welfare, the government of Japan.

[2] Address correspondence and reprint requests to Dr. Masafumi Takiguchi, Division of Viral Immunology, Center for AIDS Research, Kumamoto University, 2-2-1 Honjo, Kumamoto 860-0811, Japan. E-mail address: masafumi@kaiju.medic.kumamoto-u.ac.jp

0022-1767/04/$02.00

HLA-class I tetramers

HLA-class I-peptide tetrameric complexes (tetramers) were synthesized as previously described (14). The human CMV (HCMV)[3] CTL epitope (HCMV-1 $pp65_{495-503}$, NLVPMVATV; Ref. 15) and the EBV CTL epitope (EBV 3B 399–408, AVFDRKSDAK; Ref. 16) were used for refolding of HLA-A*0201 or HLA-A*0206 molecules and HLA-A*1101 molecules, respectively. PE-labeled streptavidin (Molecular Probes, Eugene, OR) or allophycocyanin-Cy7-labeled streptavidin (Cedarlane Laboratories, Hornby, Ontario, Canada) was used for generation of tetramers.

Flow cytometric analysis

PBMCs from healthy individuals were stained with anti-CD3 mAb, anti-CD8 mAb, and anti-CXCR1 mAb or anti-CXCR2 mAb. The cells were incubated at 4°C for 30 min, and were then washed two times with PBS containing 10% newborn cow serum (PBS/10% NCS). The percentage of $CXCR1^+CD8^+$ T cells in the total $CD8^+$ T cells was determined by using a FACSCalibur (BD Biosciences, San Jose, CA). Furthermore, to clarify CXCR1 expression in each CD27CD28CD45RA subset of total $CD8^+$ T cells, we purified $CD8^+$ T cells from PBMC by using anti-CD8-coated magnetic beads (Miltenyi Biotec, Bergisch Gladbach, Germany). The percentage of $CD8^+$ T cells among the purified cells was >98%. Purified $CD8^+$ T cells were stained with anti-CD27 mAb, anti-CD28 mAb, anti-CD45RA mAb, and anti-CXCR1 mAb. The cells were incubated at 4°C for 30 min, and were then washed two times with PBS/10% NCS. The percentage of $CXCR1^+$ cells in each subset was measured by using the FACSCalibur.

To define intracellular perforin expression in $CXCR1^+$ and $CXCR1^-$ subsets of total $CD8^+$ T cells, we stained PBMCs with anti-CD8 mAb and anti-CXCR1 mAb, fixed them in 4% paraformaldehyde at 4°C for 20 min, and then permeabilized them at 4°C for 10 min with PBS containing with 0.1% saponin and 20% NCS (permeabilizing buffer). The cells were washed with permeabilizing buffer and then resuspended in 50 μl of the same buffer. After anti-perforin mAb had been added, the cell suspension was incubated at 4°C for 30 min, and the cells were then washed three times in the permeabilizing buffer at 4°C. PE-labeled mouse IgG1 was used as a negative control.

To determine the expression of CXCR1 on HCMV-specific and EBV-specific $CD8^+$ T cells, we purified $CD8^+$ T cells and mixed them with HCMV-1-A*0201, HCMV-1-A*0206 or EBV-1-A*1101 tetramers at a concentration of 0.02–0.04 mg/ml. After incubation at 37°C for 30 min, the cells were washed two times with RPMI 1640/10% NCS, and then anti-CXCR1 mAb only or anti-CD27 mAb, anti-CD28 mAb, anti-CD45RA mAb, and anti-CXCR1 mAb were added to the cell suspension. The cells were incubated at 4°C for 30 min, and were then washed two times with PBS/10% NCS.

Assay for cytotoxic activity

Cytotoxic activity was measured by the standard ^{51}Cr-release assay as follows. Target cells (2×10^5) were incubated for 60 min with 100 μCi $Na_2{}^{51}CrO_4$ in saline and washed three times with RPMI 1640/10% NCS. Labeled target cells (2×10^3/well) were added to U-bottom 96-well plates with the corresponding peptide (10^{-6} M). After 1 h incubation, $CD8^+$ T cells purified by anti-CD8 mAb-coated beads or $CXCR1^+CD8^+$ T cells purified by a cell sorter (FACSAria; BD Biosciences) were added, and the mixtures were then incubated for 6 h at 37°C. The supernatants were then collected and analyzed with a gamma counter.

Lymphocyte chemotaxis assay

The lymphocyte chemotaxis assay was performed by using 96-well microchemotaxis chambers (NeuroProbe, Gaithersburg, MD) as follows. The $CD8^+$ T cells or $CXCR1^-CD8^+$ T cells purified by a cell sorter (5×10^5 cells/well) were placed over the filter (5-μm pore diameter) in the upper wells of the chamber. Recombinant human IL-8 (BD Biosciences) was diluted with RPMI 1640 and then applied to the lower wells of the chamber. After incubation at 37°C for 3 h, the cells that had migrated through the filter were collected by centrifugation and counted. The data were expressed as the average number of cells that had migrated in three wells. The cells that had migrated nonspecifically were excluded.

Results and Discussion

A previous study showed that IL-8 receptors CXCR1 and CXCR2 were expressed on the surface of some $CD8^+$ T cells (13). To confirm this, we investigated the surface expression of CXCR1 and CXCR2 on total $CD8^+$ T cells. We first examined their surface expression on PBMC by using anti-CXCR1 and anti-CXCR2 mAbs. $CXCR1^+$ cells were detected among both small-size (lymphocytes) and large-size (monocytes) cells, whereas $CXCR2^+$ cells were found only among the latter (Fig. 1*A*). These results support a previous finding that both IL-8 receptors are expressed on monocytes (10), and suggest that only CXCR1 is expressed on T cells. To clarify the expression of these receptors on T cells, we examined the CXCR1 and CXCR2 expression on T cells among PBMCs from healthy individuals by using anti-CD3, anti-CD8, and anti-CXCR1 or anti-CXCR2 mAbs. A representative result is shown in Fig. 1*B*. A significant number of $CD8^+$ T cells expressed CXCR1, whereas almost no $CD8^+$ T cells expressed CXCR2 (Fig. 1*B*). In contrast, $CD8^-$ T cells did not express CXCR1 (data not shown). The lack of CXCR2 expression on $CD8^+$ T cells was confirmed by examining the cells from nine healthy individuals. The expression of CXCR1 varied among these nine individuals, with the percentage of $CXCR1^+CD8^+$ T cells among the total $CD8^+$ T cells ranging from 7.6 to 51.0% (mean ± SD, 22.6 ± 15.6%; Fig. 1*C*). These results indicate that a given subset of $CD8^+$ T cells expresses CXCR1, but are in conflict with a previous finding that $CD8^+$ T cells express CXCR2 (10).

Our recent study showed that naive, memory, and effector $CD8^+$ T cell subsets can be classified by CD27, CD28, and CD45RA (4). Therefore, we investigated the surface expression of CXCR1 on each CD27CD28CD45RA subset in the total $CD8^+$ T cells. Total $CD8^+$ T cells were isolated from PBMC of 10 healthy individuals, and then analyzed by four-color flow cytometric analysis with anti-CD27, anti-CD28, anti-CD45RA, and anti-CXCR1 mAb. CXCR1-positive cells were found in subsets with $CD27^-CD28^-CD45RA^{+/-}$ and

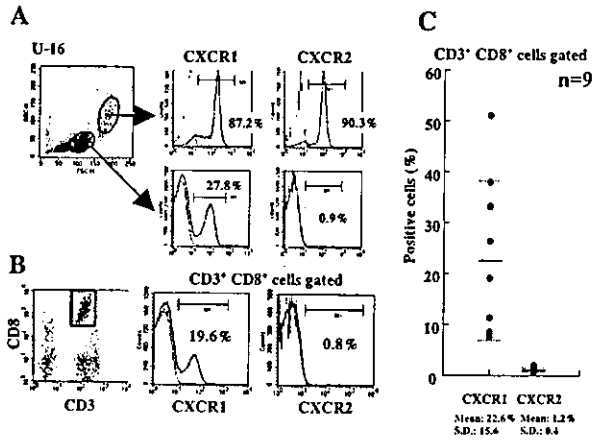

FIGURE 1. Surface expression of CXCR1 on $CD8^+$ T cells. *A*, Surface expression of CXCR1 and CXCR2 on PBMC. PBMCs from a given individual (U16) were stained with anti-CXCR1 or -CXCR2 mAb. Frequency of $CXCR1^+$ and of $CXCR2^+$ cells in both small- and large-size cell populations was analyzed by flow cytometry. The percentage of $CXCR1^+$ or $CXCR2^+$ cells is given in each plot. *B*, Surface expression of CXCR1 and CXCR2 on $CD8^+$ T cells. PBMC from individual U16 were stained with anti-CD3, anti-CD8, and anti-CXCR1 or anti-CXCR2 mAbs. The $CD3^+CD8^+$ subset was gated, and then the surface expression of CXCR1 and of CXCR2 was analyzed. The percentage of $CXCR1^+$ cells or $CXCR2^+$ cells is given in each plot. *C*, Variation of CXCR1 and CXCR2 expression on $CD8^+$ T cells in nine healthy individuals. The mean percentage and SD of $CXCR1^+$ cells and $CXCR2^+$ cells in the $CD3^+CD8^+$ subset are presented in the figures.

[3] Abbreviations used in this paper: HCMV, human CMV; GCP, granulocyte chemotactic protein; MFI, mean fluorescence intensity; NCS, newborn cow serum.